

# Visual-ERM: Reward Modeling for Visual Equivalence

Ziyu Liu<sup>\*1,2</sup>, Shengyuan Ding<sup>\*2,3</sup>, Xinyu Fang<sup>2</sup>, Xuanlang Dai<sup>2</sup>, Penghui Yang<sup>2</sup>, Jianze Liang<sup>2</sup>, Jiaqi Wang<sup>2</sup>, Kai Chen<sup>2</sup>, Dahua Lin<sup>2,4</sup> and Yuhang Zang<sup>†2</sup>

<sup>1</sup>Shanghai Jiao Tong University, <sup>2</sup>Shanghai AI Laboratory, <sup>3</sup>Fudan University, <sup>4</sup>CUHK

Vision-to-code tasks require models to reconstruct structured visual inputs, such as charts, tables, and SVGs, into executable or structured representations with high visual fidelity. While recent Large Vision Language Models (LVLMs) achieve strong results via supervised fine-tuning, reinforcement learning remains challenging due to misaligned reward signals. Existing rewards either rely on textual rules or coarse visual embedding similarity, both of which fail to capture fine-grained visual discrepancies and are vulnerable to reward hacking. We propose Visual Equivalence Reward Model (**Visual-ERM**), a multimodal generative reward model that provides fine-grained, interpretable, and task-agnostic feedback to evaluate vision-to-code quality directly in the rendered visual space. Integrated into RL, **Visual-ERM** improves Qwen3-VL-8B-Instruct by +8.4 on chart-to-code and yields consistent gains on table and SVG parsing (+2.7, +4.1 on average), and further strengthens test-time scaling via reflection and revision. We also introduce VisualCritic-RewardBench (VC-RewardBench), a benchmark for judging fine-grained image-to-image discrepancies on structured visual data, where **Visual-ERM** at 8B decisively outperforms Qwen3-VL-235B-Instruct and approaches leading closed-source models. Our results suggest that fine-grained visual reward supervision is both necessary and sufficient for vision-to-code RL, regardless of task specificity.

## 1. Introduction

Large Vision Language Models (LVLMs) have achieved impressive advances in multimodal understanding [2, 9, 22]. Among their emerging capabilities, vision-to-code has emerged as particularly impactful: it converts structured visual inputs (e.g., charts, tables, SVGs) into executable or structured representations like code [41] or markdown [21]. Vision-to-code has become a key primitive for downstream systems, enabling diverse applications, including AI-assisted front-end development (converting UI designs to code) [28], scientific paper parsing, and facilitating knowledge management and system integration.

Most existing approaches improve vision-to-code through supervised fine-tuning (SFT) [41, 42]. However, SFT is data-intensive, requiring substantial annotation effort across diverse tasks, while learned models often lack cross-domain generalization. Recently, reinforcement learning (RL) has emerged as a promising alternative [15, 32], but it introduces new challenges: the need for **reliable reward supervision**. As shown in the left part of Fig. 1, existing reward approaches fall into two camps. Text-based metrics such as edit distance and Tree Edit Distance Similarity (TEDS) operate purely in the textual domain, missing critical visual cues like alignment, spacing, and layout errors, leaving room for reward hacking. In contrast, vision-encoder rewards (e.g., DINO [4]) are coarse-grained and semantically-biased, insensitive to fine-grained visual details essential for parsing tasks. Additionally, both reward methods are vulnerable to reward hacking: as illustrated in Fig. 1, an output can achieve a very high reward score (e.g., DINO similarity of 0.99) while still containing substantial parsing errors. Both approaches provide brittle, exploitable reward signals inadequate for vision-to-code RL training.

These limitations call for a fundamentally different approach: reward models must use both textual and visual evidence in a unified cross-modal space, sensitive to visual fidelity at multiple scales from global structure

† Corresponding authors: Yuhang Zang (zangyuhang@pjlab.org.cn)

\* Equal contribution. Code is at <https://github.com/InternLM/Visual-ERM>

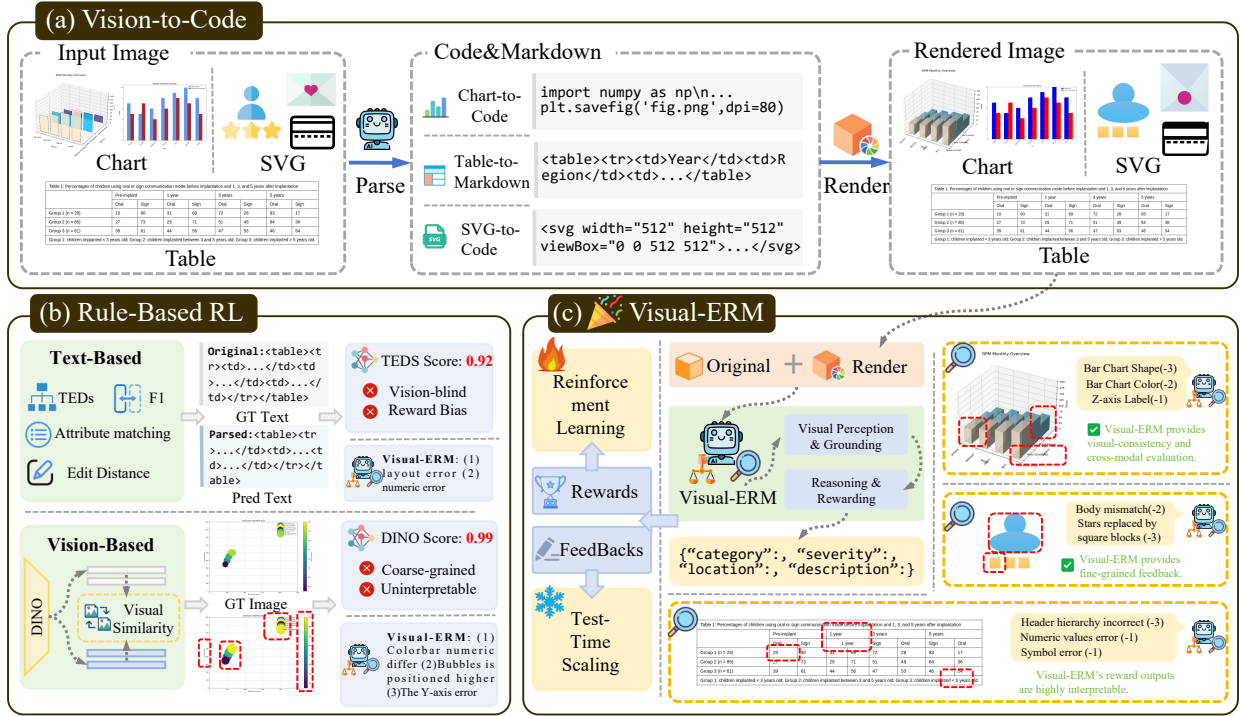


**Figure 1: Overview of vision-to-code reward modeling and Visual-ERM.** (a) Vision-to-code transforms structured visual inputs (charts, tables, and SVGs) into structured textual outputs (code or markup). Rendering the predicted text back into an image enables evaluation in the visual space. (b) Prior rewards either rely on text-based rule metrics, which ignore critical visual cues, or use vision-encoder feature similarity, which is coarse-grained and lacks interpretability. (c) Visual-ERM provides fine-grained, interpretable, and task-agnostic reward signals for vision-to-code, serving as a reliable supervisor in both RL pipelines and test-time scaling.

to pixel-level details. Such a model must jointly perceive visual details, read embedded text, and reason about structural fidelity beyond semantic similarity.

To address this, we propose the Visual Equivalence Reward Model (Visual-ERM), a multimodal generative reward model for vision-to-code. By jointly modeling global structure and local visual details, Visual-ERM provides reward signals with three key properties: (i) **Fine-grained**: it captures subtle visual discrepancies beyond coarse semantic similarity; (ii) **Interpretable**: it produces diagnostic feedback that can guide reflection and revision for test-time scaling; (iii) **Task-agnostic**: a single RM generalizes across chart-to-code, table-to-markdown and SVG-to-code. This enables substantially stronger supervision than text-based metrics or vision-encoder similarity, providing faithful guidance toward true visual equivalence.

To measure reward model quality directly, we introduce VisualCritic-RewardBench (VC-RewardBench), a benchmark for assessing fine-grained image-to-image discrepancy judgment across charts, tables, and SVGs. On VC-RewardBench, Visual-ERM achieves strong performance despite its 8B scale, decisively outperforming Qwen3-VL-235B-Instruct and approaching leading closed-source models.

We also evaluate Visual-ERM by integrating it into RL pipelines across existing vision-to-code benchmarks: chart-to-code (ChartMimic [35]), table-to-markdown (OmniDocBench [23], olmOCRbench [25]), and SVG-to-code (UniSVG [12]). Results demonstrate substantial improvements: Visual-ERM boosts Qwen3-VL-8B-Instruct by +8.4 points on chart-to-code (outperforming DINO-based rewards) and delivers consistent gains on table and SVG parsing (+2.7 and +4.1 points respectively). We further apply Visual-ERM to test-time scaling, where it enables reflection and revision to yield additional improvements in parsing accuracy.

In summary, our contributions are as follows:

1) We propose the Visual Equivalence Reward Model (Visual-ERM), a multimodal generative reward model that provides fine-grained, interpretable, and task-agnostic reward signals for vision-to-code, and can be seamlessly integrated into both RL pipelines and test-time scaling.

2) We provide a systematic analysis of reward design limitations for vision-to-code, demonstrating that text-based metrics and vision-encoder similarity are both inadequate for faithful visual assessment.

3) We introduce VisualCritic-RewardBench, a benchmark for evaluating fine-grained image-to-image discrepancy judgment across structured visual data (charts, tables, SVGs).

4) We demonstrate that Visual-ERM enables effective RL across multiple vision-to-code tasks, improving Qwen3-VL-8B-Instruct by +8.4 points on chart-to-code and yielding consistent gains on table-to-markdown and SVG-to-code (+2.7 and +4.1 on average); Visual-ERM further strengthens test-time scaling via reflection and revision.

## 2. Related Works

**Reward Models.** To enable effective RL [16, 27], reward models (RMs) provide feedback that guide policy optimization. RMs can take several forms: (1) **Bradley–Terry (BT)** models that learn a scalar reward from pairwise comparisons and are often instantiated as discriminative rankers [3, 38, 44]; (2) **generative** RMs that produce natural language critiques or judgments which can be mapped to rewards [11, 17, 33, 37]; and (3) **thinking/agentive** RMs that perform multi-step evaluation, e.g., decomposing criteria, self-reflection, or invoking tools before returning a final score [7, 14, 24]. Most prior RMs are developed for text-centric generation (e.g., writing and dialogue) and do not support *visual-to-code* tasks, where quality is mainly determined by visual fidelity rather than text. This limitation hinders further RL improvements on visual-to-code tasks. Therefore, we propose Visual-ERM, a visual equivalence reward model for visual-to-code tasks.

**Visual-to-Code Tasks.** Visual-to-code spans a family of practical structured perception tasks that convert images into executable or structured representations. *Chart-to-Code* aims to parse charts into Python programs that can faithfully reproduce the original plots [32, 40, 42]. *Table-to-Markdown* converts tabular images into structured formats such as Markdown or HTML [15, 21, 39]. *SVG-to-Code* translates vector graphics into code representations [12, 36]. Such structured outputs facilitate downstream use and improve usability in real-world applications.

**RL for Visual-to-Code Tasks.** Despite its practical importance, visual-to-code remains challenging. Supervised fine-tuning (SFT) typically relies on large-scale, high-quality datasets [8, 42, 43], which are costly to curate. RL has been explored as an alternative, yet existing reward designs often fall into two extremes: (i) textual rule-based rewards [15], which score string level or structural proxies in the text space without directly leveraging the visual evidence, and thus may introduce modality bias; and (ii) visual encoder’s similarity-based rewards, such as DINO-based [29] similarity [32, 41], which compare representations extracted by vision encoders but are often coarse-grained and offer limited interpretability. Motivated by these limitations, we propose Visual-ERM, a cross-modal reward model that provides fine-grained, interpretable and task-agnostic feedback for Visual-to-Code.

## 3. Methods

We now present the complete pipeline for Visual-ERM. Our approach comprises three interconnected components: (i) reward data generation via controlled corruption and annotation, (ii) supervised fine-tuning of the reward model, and (iii) integration Visual-ERM into RL and test-time scaling. We also introduce VisualCritic-RewardBench to benchmark fine-grained image-to-image discrepancy judgment.

### 3.1. Visual-ERM: Data, Annotation, and Training

The training pipeline consists of three key stages shown in Fig. 2: (i) reward data generation through controlled corruption, (ii) fine-grained annotation via distillation, and (iii) supervised fine-tuning of the reward model.

**Reward Data Generation.** In vision-to-code tasks (e.g., Chart/Table/SVG-to-Code), parsing quality can be assessed either in text space or in vision space. Let  $m \in \{\text{CHART}, \text{TABLE}, \text{SVG}\}$  denote the task type. Given an input ground truth image  $I^*$  and its ground truth structured text  $y^*$ , a vision-to-code model produces a predicted structured output  $y$  (e.g., code/markdown). Text-space evaluation compares  $y$  against  $y^*$  via a

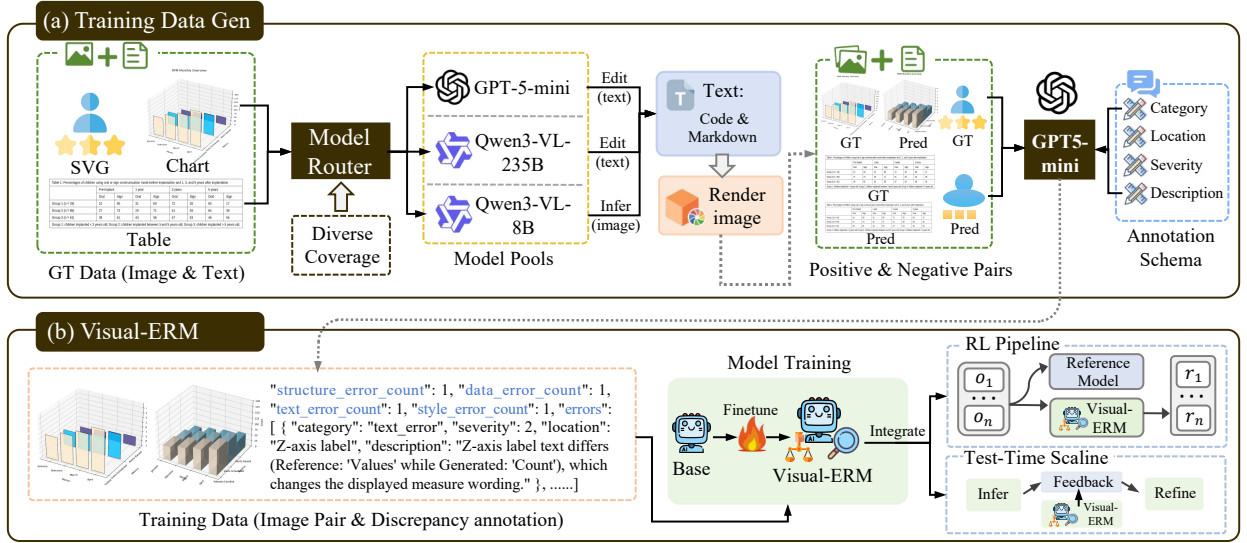


**Figure 2:** (a) **Training Data Generation.** Starting from raw images and associated text, we construct image pairs by (i) synthesizing negative samples via targeted edits that inject pre-defined error types, and (ii) sampling naturally occurring errors from direct model inference. We then obtain fine-grained annotations for each image pair using proprietary models. (b) **Visual-ERM.** We train **Visual-ERM** on the resulting data and integrate it into both RL training and test-time scaling.

text-based metric  $S_{\text{text}}(\cdot, \cdot)$ :

$$S_{\text{text}}(y, y^*), \quad (1)$$

where  $S_{\text{text}}$  can be instantiated by edit distance or other string/structure similarity measures. In contrast, vision-space evaluation renders  $y$  into an image  $\hat{I} = \mathcal{R}_m(y)$  using a specific renderer  $\mathcal{R}_m(\cdot)$ , and measures the visual fidelity between the rendered image  $\hat{I}$  and the ground-truth image  $I^*$  using a visual-space metric  $S_{\text{vis}}(\cdot, \cdot)$ :

$$S_{\text{vis}}(\hat{I}, I^*) = S_{\text{vis}}(\mathcal{R}_m(y), I^*). \quad (2)$$

**Visual-ERM** adopts the vision-space paradigm to better match human judgments of visual fidelity. Specifically, our reward model  $f_{\theta_{ERM}}$ , parameterized by  $\theta_{ERM}$ , takes  $(I^*, \hat{I})$  as input and outputs a scalar reward

$$r(I^*, y) = f_{\theta_{ERM}}(I^*, \mathcal{R}_m(y)), \quad (3)$$

where  $r(I^*, y)$  is the reward assigned to prediction  $y$  under ground truth  $I^*$ . To train **Visual-ERM**, we construct a reward dataset  $\mathcal{D}_{\text{reward}}$  consisting of annotated image pairs across tasks:  $\mathcal{D}_{\text{reward}} = \{(m, I^*, \hat{I}, a)\}$  where  $\hat{I} = \mathcal{R}_m(y)$ , and  $a$  is a fine-grained discrepancy annotation.

**Fine-grained Annotation.** As shown in Fig. 2, to obtain such image pairs, we collect open-source GT images and their corresponding textual representations. We then create corrupted structured outputs  $y$  in two complementary ways: (1) *Edit*: using strong LLMs to perturb the GT structured text and inject controlled, pre-defined error types; and (2) *Infer*: using weaker LLMs to directly make prediction, thereby sampling naturally occurring errors that better match the error distribution encountered in practice. After obtaining  $y$ , we render it into  $\hat{I}$  via  $\mathcal{R}_m(\cdot)$ , thereby forming the distorted counterpart and constructing the image pair  $(I^*, \hat{I})$ .

Next, we generate fine-grained annotations  $a$  for each image pair. We observe a substantial gap between open and closed source models in localizing image discrepancies: even very large models, such as Qwen3-VL-235B-Instruct [2], often fail to reliably pinpoint fine-grained discrepancies, as further evidenced by the results in Sec. 4.3. To ensure annotation quality while keeping the cost manageable, we adopt a distillation pipeline that transfers the strong discrepancy-localization capability of GPT-5-mini [30] into a more efficient models, enabling scalable reward generation. The procedure is illustrated in Fig. 2.

**Optimization.** We train **Visual-ERM** via supervised fine-tuning (SFT) on the reward dataset  $\mathcal{D}_{\text{reward}} = \{(m, I^*, \hat{I}, a)\}$ . Let  $f_{\theta_{ERM}}(a | x)$  denote the conditional generation distribution of **Visual-ERM** parameterized by  $\theta_{ERM}$ , where  $x = (I^*, \hat{I})$ .

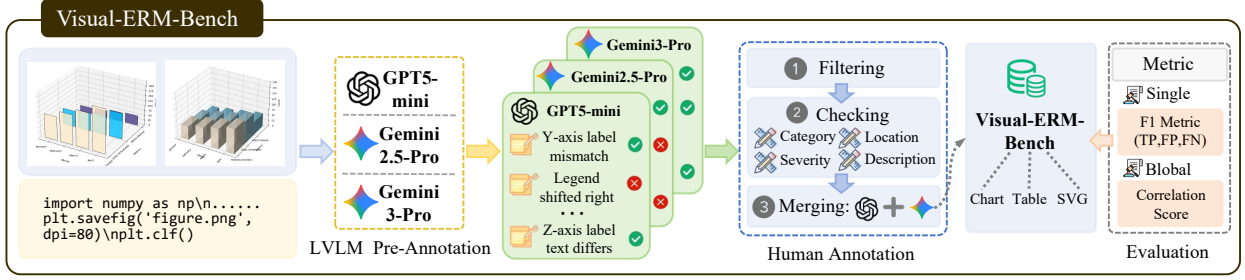


**Figure 3: VC-RewardBench.** We construct VC-RewardBench by first leveraging several advanced proprietary models for preliminary annotation, followed by manual consolidation and filtering, resulting in 1,335 high-quality instances.

We optimize **Visual-ERM** with the negative log-likelihood (NLL) objective:

$$\mathcal{L}(\theta) = \mathbb{E}_{(m, I^*, \hat{I}, a) \sim \mathcal{D}_{\text{reward}}} \left[ -\log f_{\theta_{ERM}}(a | x) \right]. \quad (4)$$

Equivalently, for an annotation sequence  $a = (a_1, \dots, a_T)$  with length  $T$ , the token-level objective is

$$\mathcal{L}(\theta) = \mathbb{E}_{(m, I^*, \hat{I}, a)} \left[ -\sum_{t=1}^T \log f_{\theta_{ERM}}(a_t | x, a_{<t}) \right], \quad (5)$$

where  $a_{<t} = (a_1, \dots, a_{t-1})$  are the preceding target tokens.

## 3.2. Visual-ERM for Reinforcement Learning

### 3.2.1. Reward Design

**Visual-ERM** serves as a reward model that provides fine-grained feedback for RL. We apply it to multiple vision-to-code tasks (Chart, Table, SVG) and optimize the policy model with a GRPO-based optimization algorithm. In each rollout, the policy model generates a textual output  $y$ , which is rendered into an image  $\hat{I} = \mathcal{R}_m(y)$ . We then feed  $(I^*, \hat{I})$  into **Visual-ERM** to obtain discrepancy predictions and severity scores. We additionally use a render-success reward (RSR) to encourage outputs that can be rendered successfully, serving a similar purpose to a format reward.

Formally, let  $\mathcal{E} = \{e_k\}_{k=1}^K$  denote the discrepancy set predicted by **Visual-ERM** for  $(I^*, \hat{I})$ , where each error  $e_k$  is associated with a severity score  $s_k \geq 0$ . We define  $S_{\text{VERM}}$  as the sum of predicted severities:

$$S_{\text{VERM}} = \sum_{k=1}^K s_k. \quad (6)$$

To map this score into  $[0, 1]$ , we normalize it by the maximum severity score ( $\max_{j \in \mathcal{T}} S_{\text{VERM}}^{(j)}$ ) within the current task  $\mathcal{T}$ :

$$\tilde{S}_{\text{VERM}} = \frac{S_{\text{VERM}}}{\max_{j \in \mathcal{T}} S_{\text{VERM}}^{(j)} + \epsilon}, \quad (7)$$

where  $\epsilon$  is a small constant for numerical stability. We then convert it to a bounded reward by

$$r_{\text{VERM}} = \text{clip}(1 - \tilde{S}_{\text{VERM}}, 0, 1). \quad (8)$$

Finally, the overall reward used in RL is:

$$r = r_{\text{RSR}} + r_{\text{VERM}}, \quad (9)$$

where  $r_{\text{RSR}}$  is the render-success reward ( $r_{\text{RSR}} = 1$  if rendering succeeds and 0 otherwise).

### 3.2.2. Optimization

We optimize the policy model with a GRPO-based RL objective, where the reward  $r(x, y)$  is defined in Eq. 9. Let  $x = I^*$  denote the policy input, where  $I^*$  is the original image, and let  $y$  denote the structured output generated by the policy. Given the policy  $\pi_\theta(y | x)$  and a reference policy  $\pi_{\text{ref}}(y | x)$ , we maximize the KL-regularized expected reward:

$$\begin{aligned} \max_{\theta} \mathbb{E}_{I^* \sim \mathcal{D}} & \left[ \mathbb{E}_{y \sim \pi_\theta(\cdot | I^*)} [r_{\text{RSR}}(\mathcal{R}_m(y)) \right. \\ & + \text{clip}(1 - \tilde{S}_{\text{VERM}}(I^*, \mathcal{R}_m(y)), 0, 1)] \\ & \left. - \beta \text{KL}(\pi_\theta(\cdot | I^*) \| \pi_{\text{ref}}(\cdot | I^*)) \right]. \end{aligned} \quad (10)$$

where  $\beta$  controls the strength of KL regularization and  $\mathcal{D}$  is the training distribution over input images  $I^*$ .

### 3.2.3. Visual-ERM for Test-Time Scaling

Another key use case of **Visual-ERM** is to provide feedback signals for test-time scaling (TTS) via iterative self-refinement. As illustrated in Fig. 2 (b), given an input  $x = I^*$ , the model first produces an initial structured prediction

$$y^{(0)} \sim \pi_\theta(\cdot | x), \quad (11)$$

which is rendered into an image  $\hat{I}^{(0)} = \mathcal{R}_m(y^{(0)})$  and evaluated by **Visual-ERM**:

$$(r^{(0)}, f^{(0)}) = f_{\theta_{\text{ERM}}}(I^*, \hat{I}^{(0)}), \quad (12)$$

where  $r^{(0)}$  denotes the estimated quality score,  $f^{(0)}$  is the fine-grained description and  $\theta_{\text{ERM}}$  is the policy of **Visual-ERM**. If the quality is unsatisfactory, the model conditions on its previous prediction and the feedback to revise the solution:  $y^{(1)} \sim \pi_\theta(\cdot | x, y^{(0)}, f^{(0)})$ . We evaluate this capability in Sec. 4.4.

## 3.3. VisualCritic-RewardBench

Most existing reward benchmarks focus on vision–language alignment (e.g., VL-RewardBench [13]), whereas benchmarks for fine-grained *image-to-image* discrepancy discrimination remain scarce. We therefore introduce VisualCritic-RewardBench (VC-RewardBench), which targets structured visuals (charts, tables, SVGs) and measures *image-to-image* alignment fidelity.

VC-RewardBench contains 1,335 high-quality annotated instances, constructed following Fig. 3. Each instance includes a ground-truth image, a corrupted counterpart, and fine-grained discrepancy annotations (type, location, description, severity). We first curated 4.5k candidate image pairs and collected three independent annotations per pair from GPT5-mini [30], Gemini-2.5-Pro, and Gemini-3-Pro [6]. PhD-level annotators then reviewed, corrected, and consolidated these annotations, yielding the final 1,335-instance benchmark. Example cases are provided in Sec. D.

VC-RewardBench requires outputs that combine structured fields (e.g., counts) with free-form content (e.g., descriptions), making exact-match accuracy unsuitable. We therefore evaluate with an *LLM-as-Judge* protocol: a judge LLM matches predicted discrepancies  $\hat{A}$  to ground-truth annotations  $A^*$  to identify TP/FP/FN and compute Precision/Recall/F1. In addition, since models also output per-discrepancy severity scores, we sum severities per instance and report the Pearson correlation with the ground-truth totals to measure overall scoring consistency, denoted as  $S_c$ .

## 4. Experiments

### 4.1. Experimental Setup

**Experimental Details** We train **Visual-ERM** on top of Qwen3-VL-8B-Instruct [1]. To assess **Visual-ERM**’s effectiveness as reward model, we perform RL on three vision-to-code tasks: (1) *Chart-to-Code*, (2) *Table-to-Markdown*, and (3) *SVG-to-Code*. We adopt GRPO [27] as our RL algorithm. For vision-to-code RL, we also adopt Qwen3-VL-8B-Instruct as the policy backbone. In addition, we include stronger parsing-oriented policy

**Table 1: Evaluation Results on Chart-to-Code Tasks.** We evaluate on ChartMimic(Direct) and ChartMimic(Customized). ChartMimic(Direct) requires generating Python code that reproduces the input chart, while ChartMimic(Customized) requires generating code for a new chart that matches the given chart’s style and data constraints. **Exec\_rate** denotes the execution success rate; **Low** and **High** denote the low-level and high-level scores, respectively.

Model	ChartMimic (Direct)				ChartMimic (Customized)				Avg↑
	Exec_rate↑	Low↑	High↑	Overall↑	Exec_rate↑	Low↑	High↑	Overall↑	
<i>Baseline</i>									
InternVL3.5-8B	62.2	41.9	48.9	45.4	79.7	53.0	63.3	58.2	51.8
Qwen3-VL-8B-Instruct	82.2	62.7	72.7	67.7	86.8	66.3	76.8	71.6	69.6
VinciCoder-8B-SFT	86.2	68.2	77.5	72.9	86.2	52.3	71.5	61.9	67.4
JanusCoderV-8B	80.6	65.8	73.2	69.5	80.7	66.7	74.2	70.4	70.0
ChartMaster-7B	93.3	74.5	82.1	78.3	88.8	59.5	74.2	66.8	72.6
<i>Qwen3-VL-8B-Instruct</i>									
+ RL (DINO-based Reward)	90.8	71.1	81.9	76.5	91.7	71.2	80.3	75.8	76.1
+ RL (Visual-ERM)	92.5	74.4	84.6	79.5	91.5	71.8	81.1	76.5	78.0
$\Delta_{vs. Qwen3-VL-8B-Instruct}$	<b>+10.3</b>	<b>+11.9</b>	<b>+11.9</b>	<b>+11.8</b>	<b>+4.7</b>	<b>+5.5</b>	<b>+4.3</b>	<b>+4.9</b>	<b>+8.4</b>
<i>VinciCoder-8B-SFT</i>									
+ RL (DINO-based Reward)	90.8	73.1	82.3	77.7	91.5	57.0	77.5	67.3	72.5
+ RL (Visual-ERM)	94.3	78.0	88.5	83.2	95.0	60.9	82.6	71.7	77.5
$\Delta_{vs. VinciCoder-8B-SFT}$	<b>+8.1</b>	<b>+9.8</b>	<b>+11.0</b>	<b>+10.3</b>	<b>+8.8</b>	<b>+8.6</b>	<b>+11.1</b>	<b>+9.8</b>	<b>+10.1</b>

model, VinciCoder [41], and JanusCoderV-8B [31] as an external baseline. More experimental details refer to Sec. A.

**Benchmarks** We evaluate three vision-to-code tasks. For *Chart-to-Code*, we use CHARTMIMIC [35] in both *direct* (reproduce the input chart) and *customized* (generate a new chart under given style/data constraints) settings. For *Table-to-Markdown*, we report table metrics on OMNIDOCBENCH-v1/v1.5 [23] and OLMOCR BENCH [25]. For *SVG-to-Code*, we evaluate on UNISVG [12].

These benchmarks measure vision-to-code parsing quality, but do not directly evaluate a model’s ability to judge reconstruction fidelity or provide discrepancy feedback. We therefore introduce VisualCritic-RewardBench, which benchmarks fine-grained discrepancy detection and actionable feedback across vision-to-code tasks.

## 4.2. Visual-ERM for Reinforcement Learning

### Results on Chart-to-Code

We first apply **Visual-ERM** to the *Chart-to-Code* task. Starting from Qwen3-VL-8B-Instruct and VinciCoder-8B-SFT, we use **Visual-ERM** to provide reward signals in GRPO training process. For comparison, we also train both models with the DINO-based RL recipe described in VinciCoder [41]. Results are reported in Tab. 1.

As shown in Tab. 1, RL guided by **Visual-ERM** substantially improves Qwen3-VL-8B-Instruct on both ChartMimic-v2-direct and ChartMimic-v2-customized [35], increasing the average score by **+11.8** and **+4.9**, respectively. Moreover, starting from the already strong VinciCoder-8B-SFT, **Visual-ERM**-guided RL still delivers consistent gains of **+10.3** and **+9.8** under the two settings.

Compared with DINO-based RL, **Visual-ERM**-guided RL yields substantially larger gains for both the Qwen3-VL-8B-Instruct and VinciCoder-8B-SFT initialized policy model. A key limitation of DINO-based rewards is that they reduce the supervision to a fixed visual embedding space: the policy is encouraged to match patch-level feature similarity, which is known to prioritize semantic alignment and global appearance while under-penalizing small but functionally critical

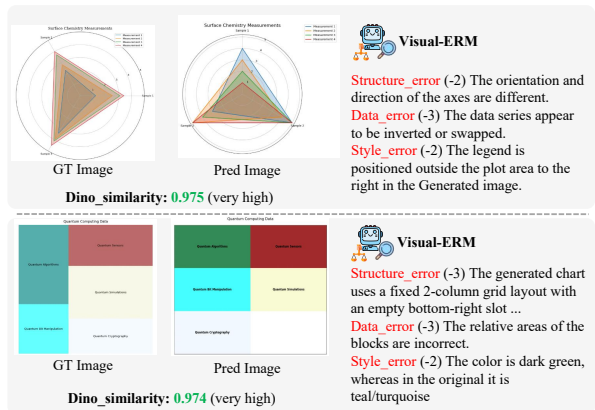


**Figure 4: DINO vs. Visual-ERM.** DINO scores are semantically-biased, which can lead to inflated rewards and reward hacking. In contrast, **Visual-ERM** accounts for fine-grained visual details and provides more precise and interpretable evaluations.

**Table 2: Evaluation Results on Table-to-Markdown.** TEDS-S denotes TEDS-Structure-Only, and TA represents the table subtask of olmOCRBench. For Edit-Dist, where lower values indicate better performance, we use  $(100 - \text{Edit-Dist})$  when computing the Average.

Model	OmniDocBench			OmniDocBench-v1.5			olmOCRBench	Avg $\uparrow$
	TEDS $\uparrow$	TEDS-S $\uparrow$	Edit-Dist $\downarrow$	TEDS $\uparrow$	TEDS-S $\uparrow$	Edit-Dist $\downarrow$	TA $\uparrow$	
<i>Baseline</i>								
Qwen2.5-VL-7B	74.4	80.1	58.9	69.3	74.1	58.7	71.1	64.5
InternVL3.5-8B	71.0	77.6	44.9	62.9	70.4	44.1	74.1	66.7
Qwen3-VL-8B-Instruct	78.9	<u>83.9</u>	<u>23.2</u>	72.7	<u>77.2</u>	<u>26.9</u>	75.3	<u>76.8</u>
<i>Qwen3-VL-8B-Instruct</i>								
+ RL (DINO-based Reward)	62.2	69.5	37.0	61.1	67.4	37.9	71.7	65.3
+ RL (TEDS-based Reward)	<u>79.2</u>	82.9	31.6	<u>73.0</u>	76.6	35.3	<b>78.6</b>	74.8
+ RL (Visual-ERM)	<b>81.4</b>	<b>86.3</b>	<b>20.7</b>	<b>75.4</b>	<b>80.4</b>	<b>24.2</b>	<u>78.1</u>	<b>79.5</b>
$\Delta_{\text{vs. Qwen3-VL-8B-Instruct}}$	<b>+2.5</b>	<b>+2.4</b>	<b>+2.5</b>	<b>+2.7</b>	<b>+3.2</b>	<b>+2.7</b>	<b>+2.8</b>	<b>+2.7</b>

deviations. Consequently, DINO-based rewards may optimize a proxy objective that does not faithfully reflect human-perceived visual fidelity.

In addition, DINO-based rewards are inherently unimodal and therefore weak at capturing errors dominated by textual content. This omission can systematically bias the reward signal, allowing policies to improve the proxy reward while degrading text faithfulness, a typical manifestation of reward hacking under proxy supervision. In contrast, **Visual-ERM** explicitly integrates visual perception with cross-modal grounding and reasoning, allowing it to evaluate reconstructions using both visual structure and rendered text. This yields a higher-fidelity reward that better correlates with the end objective and provides more informative gradients for RL optimization. A case is shown in Fig. 4 to illustrate this phenomenon.

Finally, **Visual-ERM** is trained as a generative judge, enabling it to produce fine-grained and interpretable feedback rather than a single scalar reward. Such decomposed supervision not only stabilizes RL training, but also naturally supports test-time scaling (TTS) via reward-guided refinement. We report the corresponding TTS results in Sec. 4.4.

**Results on Table-to-Markdown Parsing** We further evaluate on the *Table-to-Markdown* task. Starting from Qwen3-VL-8B-Instruct, we perform RM-based RL using **Visual-ERM**, and compare against rule-based RL using either Tree-EditDistance-based Similarity (TEDS) or DINO similarity as the reward signal. The results are reported in Tab. 2.

As shown in Tab. 2, rule-based rewards exhibit pronounced bias and reward-hacking behaviors. With a TEDS-based reward, the training reward increases steadily, yet the resulting policy improves only marginally on the target TEDS metric and slightly degrades on other metrics. We attribute this to a modality mismatch: TEDS operates purely in the textual/structural space and does not leverage visual cues, leaving ample room for the policy to exploit shortcuts that hacking the reward score.

A similar issue arises with DINO-based RL. However, unlike chart, where DINO features still capture some useful visual cues, tables are dominated by precise text content and layout constraints. As a result, DINO-based RL not only fails to yield gains on *Table-to-Markdown*, but also leads to pronounced performance degradation across benchmarks.

In contrast, **Visual-ERM**-based RL achieves consistent improvements, yielding an overall gain of **+2.7**. Benefiting from **Visual-ERM**'s multi-aspect, cross-modal, and fine-grained feedback, the resulting RL policy improves both textual recognition and structural reconstruction, indicating a better understanding of rendered table fidelity.

Model	UniSVG (ISVGEN)			
	SSIM $\uparrow$	LPIPS $\downarrow$	CLIP $\uparrow$	Score $\uparrow$
<i>Baseline</i>				
Qwen3-VL-8B	60.9	60.0	73.3	64.2
JanusCoderV-8B	58.1	61.7	72.6	62.8
VinciCoder-8B-SFT	81.1	19.2	92.5	87.9
<i>Qwen3-VL-8B-Instruct</i>				
+ RL (DINO-based Reward)	62.7	47.1	79.9	71.0
+ RL (Visual-ERM)	<b>64.4</b>	<b>52.2</b>	<b>76.5</b>	<b>68.3</b>
$\Delta_{\text{vs. Qwen3-VL-8B-Instruct}}$	<b>+3.4</b>	<b>+7.8</b>	<b>+3.1</b>	<b>+4.1</b>
<i>VinciCoder-8B-SFT</i>				
+ RL (DINO-based Reward)	76.9	23.3	92.7	86.3
+ RL (Visual-ERM)	<b>85.2</b>	<b>12.6</b>	<b>95.2</b>	<b>91.6</b>
$\Delta_{\text{vs. VinciCoder-8B-SFT}}$	<b>+4.1</b>	<b>+6.6</b>	<b>+2.7</b>	<b>+3.7</b>

**Table 3: Results on UniSVG.** SSIM and LPIPS measure pixel-level and perceptual similarity between rendered and reference SVGs, CLIP assesses semantic alignment, and **Score** is the aggregated overall metric.

**Table 4: Evaluation Results on Visual-ERM-Bench.** We evaluate a range of proprietary and open-source models on Visual-ERM-Bench.  $F1_h$  denotes  $F1_{hard}$ , the strict-match F1 score;  $F1_s$  denotes  $F1_{soft}$ , the soft-match F1 score; and  $S_c$  denotes the correlation score, measuring the overall agreement between the predicted scores and the ground-truth labels.

Model	Chart			Table			SVG			AVG		
	$F1_h$	$F1_s$	$S_c$									
<i>Proprietary</i>												
GPT-4o	22.8	28.3	48.5	32.9	35.7	49.5	13.0	19.3	50.3	25.0	29.5	56.5
GPT-5.2	30.1	32.6	64.8	39.3	40.6	54.6	28.5	32.2	61.1	32.7	35.0	58.9
Gemini-2.5-Pro	33.7	37.5	61.8	46.4	48.0	49.9	29.3	34.3	63.3	37.8	40.9	59.1
Gemini-3-Flash	38.5	41.3	62.8	48.1	50.1	45.6	33.3	67.5	64.3	40.6	43.4	53.4
<i>Open-source</i>												
Qwen2.5-VL-7B	3.9	5.4	11.2	2.3	3.1	12.6	1.9	7.5	37.9	2.8	5.1	15.2
InternVL3.5-8B	2.5	5.7	11.0	9.9	10.9	31.7	6.1	13.1	48.9	6.7	9.6	32.5
Qwen3-VL-8B-Instruct	3.3	3.5	3.8	7.0	7.8	21.4	6.1	9.4	27.1	5.3	6.5	17.5
Qwen3-VL-235B-Instruct	28.0	31.8	47.2	35.7	37.4	56.2	19.4	22.8	51.5	29.5	32.4	56.2
Visual-ERM	39.9	42.8	61.2	56.4	57.6	74.8	28.3	32.6	59.6	42.1	44.7	58.4
$\Delta_{vs. Qwen3-VL-8B-Instruct}$	<b>+36.6</b>	<b>+39.3</b>	<b>+57.4</b>	<b>+49.4</b>	<b>+49.8</b>	<b>+53.4</b>	<b>+22.2</b>	<b>+23.2</b>	<b>+32.5</b>	<b>+36.8</b>	<b>+38.2</b>	<b>+40.9</b>

Model	ChartMimic (Direct)				ChartMimic (Customized)				Avg $\uparrow$
	Exec_rate $\uparrow$	Low $\uparrow$	High $\uparrow$	Overall $\uparrow$	Exec_rate $\uparrow$	Low $\uparrow$	High $\uparrow$	Overall $\uparrow$	
Qwen3-VL-8B-Instruct	82.2	62.7	72.7	67.7	86.8	66.3	76.8	71.6	69.6
+ Reflection ( <i>w</i> Qwen3-VL-8B-Instruct)	76.2	56.8	67.1	61.9	85.5	63.8	75.2	69.5	65.7
+ Reflection ( <i>w</i> Visual-ERM)	89.8	70.3	81.0	75.6	93.2	74.0	85.1	79.5	77.6
Qwen3-VL-8B-Instruct (+RL on Visual-ERM)	92.5	74.4	84.6	79.5	91.5	71.8	81.1	76.5	78.0
+ Reflection ( <i>w</i> Qwen3-VL-8B-Instruct)	88.3	69.9	80.6	75.2	93.3	70.3	83.5	76.9	76.1
+ Reflection ( <i>w</i> Visual-ERM)	92.3	74.8	85.8	80.3	94.7	77.1	86.8	82.0	81.1

**Table 5: Test-Time Scaling.** We evaluate TTS on the *Chart-to-Code* task. Leveraging Visual-ERM as an evaluator, the model performs multiple rounds of self-reflection and revision, leading to improved parsing performance.

### Results on SVG-to-Code Parsing

We conduct the same set of experiments on the *SVG-to-Code* task. We choose Qwen3-VL-8B-Instruct and VinciCoder-8B-SFT as policy model. As a rule-based reward baseline, we apply DINO-based RL strategy. The results are summarized in Tab. 3.

Compared with chart and table, SVG reconstruction relies more heavily on visual geometry and styling cues, and is less dominated by textual content. As shown in Tab. 3, Visual-ERM-based RL yields consistent gains across backbones. In contrast, DINO-based RL improves the weaker Qwen3-VL-8B-Instruct policy but degrades performance when applied to the stronger VinciCoder-8B-SFT. This suggests that DINO-based rewards offer limited benefit that diminishes as the policy becomes stronger, whereas Visual-ERM provides robust improvements largely independent of the policy backbone.

### 4.3. Results on VC-RewardBench

To assess Visual-ERM more directly, we introduce VC-RewardBench, which evaluates both general LLMs and reward models on fine-grained discrepancy detection and reconstruction quality judgment for vision-to-code tasks. Results in Tab. 4 show that Visual-ERM (built on Qwen3-VL-8B-Instruct) substantially outperforms the baseline, improving  $F1_h/F1_s/S_c$  by **+36.8/+38.2/+40.9**. Notably, even Qwen3-VL-235B-Instruct struggles with fine-grained visual and textual discrepancies, whereas Visual-ERM markedly improves this capability, reaching performance comparable to leading proprietary systems. This indicates that Visual-ERM effectively specializes a general-purpose LLM for fine-grained discrepancy detection and fidelity judgment.

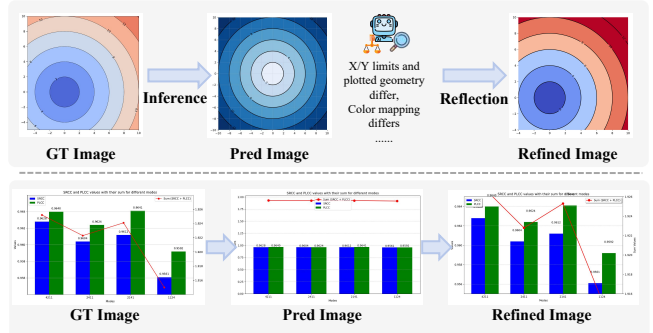


**Figure 5: Test-Time Scaling Cases.** Leveraging Visual-ERM’s fine-grained feedback, we enable an inference, reflection and refinement loop at test time. Predictions are generated as text and rendered as images for visualization.

#### 4.4. Ablation Studies

**Test-Time-Scaling** The value of [Visual-ERM](#) extends beyond serving as a reward model for RL. It can also provide fine-grained, interpretable feedback for model reflection, enabling TTS to further refine reconstruction outputs. Therefore, we incorporate [Visual-ERM](#) into the inference loop: [Visual-ERM](#) critiques each candidate, and the policy model updates its output accordingly.

As shown in Tab. 5, integrating [Visual-ERM](#) into the test-time scaling pipeline brings additional gains of **+8.0** for the base Qwen3-VL-8B-Instruct and **+3.1** for the RL-tuned model with three reflection rounds. Qualitative cases are in Fig. 5, and additional TTS ablations are reported in Sec. B.6. *Due to limited space, more experiments refer to Sec. B.*

## 5. Conclusion

We propose the Visual Equivalence Reward Model ([Visual-ERM](#)), a generative reward model that evaluates vision-to-code outputs in visual space, providing fine-grained, interpretable, and task-agnostic supervision. This addresses the fundamental limitations of prior text-based and vision-encoder similarity rewards, which are prone to modality bias and introduce reward hacking during optimization. We further introduce VisualCritic-RewardBench to directly assess image-to-image discrepancy judgment across vision-to-code tasks. Experiments show that [Visual-ERM](#) is an effective supervisor for both reinforcement learning and test-time scaling, consistently improving vision-to-code performance across multiple tasks.

## References

- [1] Shuai Bai, Yuxuan Cai, Ruizhe Chen, Keqin Chen, Xiong-Hui Chen, Zesen Cheng, Lianghao Deng, Wei Ding, Rongyao Fang, Chang Gao, Chunjiang Ge, Wenbin Ge, Zhifang Guo, Qidong Huang, Jie Huang, Fei Huang, Binyuan Hui, Shutong Jiang, Zhaohai Li, Mingsheng Li, Mei Li, Kaixin Li, Zicheng Lin, Junyang Lin, Xuejing Liu, Jiawei Liu, Chenglong Liu, Yang Liu, Dayiheng Liu, Shixuan Liu, Dunjie Lu, Ruilin Luo, Chenxu Lv, Rui Men, Li Ying Meng, Xuancheng Ren, Xin yi Ren, Sibao Song, Yu-Chen Sun, Jun Tang, Jianhong Tu, Jianqiang Wan, Peng Wang, Pengfei Wang, Qiuyue Wang, Yuxuan Wang, Tianbao Xie, Yihe Xu, Haiyang Xu, Jin Xu, Zhibo Yang, Mingkun Yang, Jianxin Yang, An Yang, Bowen Yu, Fei Zhang, Hang Zhang, Xi Zhang, Botao Zheng, Humen Zhong, Jingren Zhou, Fanxi Zhou, Jingren Zhou, Yuanzhi Zhu, and Keming Zhu. Qwen3-vl technical report. *ArXiv*, abs/2511.21631, 2025. [4.1](#)
- [2] Shuai Bai, Yuxuan Cai, Ruizhe Chen, Keqin Chen, Xionghui Chen, Zesen Cheng, Lianghao Deng, Wei Ding, Chang Gao, Chunjiang Ge, Wenbin Ge, Zhifang Guo, Qidong Huang, Jie Huang, Fei Huang, Binyuan Hui, Shutong Jiang, Zhaohai Li, Mingsheng Li, Mei Li, Kaixin Li, Zicheng Lin, Junyang Lin, Xuejing Liu, Jiawei Liu, Chenglong Liu, Yang Liu, Dayiheng Liu, Shixuan Liu, Dunjie Lu, Ruilin Luo, Chenxu Lv, Rui Men, Lingchen Meng, Xuancheng Ren, Xingzhang Ren, Sibao Song, Yuchong Sun, Jun Tang, Jianhong Tu, Jianqiang Wan, Peng Wang, Pengfei Wang, Qiuyue Wang, Yuxuan Wang, Tianbao Xie, Yiheng Xu, Haiyang Xu, Jin Xu, Zhibo Yang, Mingkun Yang, Jianxin Yang, An Yang, Bowen Yu, Fei Zhang, Hang Zhang, Xi Zhang, Bo Zheng, Humen Zhong, Jingren Zhou, Fan Zhou, Jing Zhou, Yuanzhi Zhu, and Ke Zhu. Qwen3-vl technical report. *arXiv preprint arXiv:2511.21631*, 2025. [1](#), [3.1](#), [A.1](#)
- [3] Zheng Cai, Maosong Cao, Haojiong Chen, Kai Chen, Keyu Chen, Xin Chen, Xun Chen, Zehui Chen, Zhi Chen, Pei Chu, Xiao wen Dong, Haodong Duan, Qi Fan, Zhaoye Fei, Yang Gao, Jiaye Ge, Chenya Gu, Yuzhe Gu, Tao Gui, Aijia Guo, Qipeng Guo, Conghui He, Yingfan Hu, Ting Huang, Tao Jiang, Penglong Jiao, Zhen Jin, Zhikai Lei, Jiaxing Li, Jingwen Li, Linyang Li, Shuaibin Li, Wei Li, Yining Li, Hong wei Liu, Jiangning Liu, Jiawei Hong, Kaiwen Liu, Kui-Jie Liu, Xiaoran Liu, Chen Lv, Haijun Lv, Kai Lv, Li Ma, Runyuan Ma, Zerun Ma, Wenchang Ning, Linke Ouyang, Jiantao Qiu, Yuan Qu, Fukai Shang, Yunfan Shao, Demin Song, Zifan Song, Zhihao Sui, Peng Sun, Yu Sun, Huanze Tang, Bin Wang, Guoteng Wang, Jiaqi Wang, Jiayu Wang, Rui Wang, Yudong Wang, Ziyi Wang, Xing Wei, Qizhen Weng, Fan Wu, Yingtong Xiong, Chao Xu, Rui Ze Xu, Hang Yan, Yirong Yan, Xiaogui Yang, Haochen Ye, Huaiyuan Ying, Jia Yu, Jing Yu, Yuhang Zang, Chuyu Zhang, Li Zhang, Pan Zhang, Peng Zhang, Ruijie Zhang, Shuo Zhang, Songyang Zhang, Wenjian Zhang, Wenwei Zhang, Xingcheng Zhang, Xinyue Zhang, Hui Zhao, Qian Zhao, Xiaomeng Zhao, Fen-Fang Zhou, Zaida Zhou, Jingming Zhuo, Yi-Ling Zou, Xipeng Qiu, Yu Qiao, and Dahua Lin. Internlm2 technical report. *ArXiv*, abs/2403.17297, 2024. [2](#)
- [4] Mathilde Caron, Hugo Touvron, Ishan Misra, Hervé Jégou, Julien Mairal, Piotr Bojanowski, and Armand Joulin. Emerging properties in self-supervised vision transformers. In *ICCV*, 2021. [1](#)
- [5] Lei Chen, Xuanle Zhao, Zhixiong Zeng, Jing Huang, Liming Zheng, Yufeng Zhong, and Lin Ma. Breaking the sft plateau: Multimodal structured reinforcement learning for chart-to-code generation. *arXiv preprint arXiv:2508.13587*, 2025. [A.2](#)
- [6] Gheorghe Comanici, Eric Bieber, Mike Schaekermann, Ice Pasupat, Noveen Sachdeva, Inderjit Dhillon, Marcel Blistein, Ori Ram, Dan Zhang, Evan Rosen, et al. Gemini 2.5: Pushing the frontier with advanced reasoning, multimodality, long context, and next generation agentic capabilities. *arXiv preprint arXiv:2507.06261*, 2025. [3.3](#)
- [7] Shengyuan Ding, Xinyu Fang, Ziyu Liu, Yuhang Zang, Yuhang Cao, Xiangyu Zhao, Haodong Duan, Xiaoyi Dong, Jianze Liang, Bin Wang, et al. Arm-thinker: Reinforcing multimodal generative reward models with agentic tool use and visual reasoning. *arXiv preprint arXiv:2512.05111*, 2025. [2](#)
- [8] Yi Gui, Zhen Li, Yao Wan, Yemin Shi, Hongyu Zhang, Bohua Chen, Yi Su, Dongping Chen, Siyuan Wu, Xing Zhou, et al. Webcode2m: A real-world dataset for code generation from webpage designs. In *Proceedings of the ACM on Web Conference 2025*, pages 1834–1845, 2025. [2](#)
- [9] Aaron Jaech, Adam Kalai, Adam Lerer, Adam Richardson, Ahmed El-Kishky, Aiden Low, Alec Helyar, Aleksander Madry, Alex Beutel, Alex Carney, et al. Openai o1 system card. *arXiv:2412.16720*, 2024. [1](#)

- [10] Lingjie Jiang, Shaohan Huang, Xun Wu, Yixia Li, Dongdong Zhang, and Furu Wei. Viscodex: Unified multimodal code generation via merging vision and coding models. *arXiv preprint arXiv:2508.09945*, 2025. [A.2](#)
- [11] Dahyun Kim, Chanjun Park, Sanghoon Kim, Wonsung Lee, Wonho Song, Yunsu Kim, Hyeonwoo Kim, Yungi Kim, Hyeonju Lee, Jihoo Kim, Changbae Ahn, Seonghoon Yang, Sukyung Lee, Hyunbyung Park, Gyoungjin Gim, Mikyoung Cha, Hwalsuk Lee, and Sunghun Kim. Solar 10.7b: Scaling large language models with simple yet effective depth up-scaling. *ArXiv*, abs/2312.15166, 2023. [2](#)
- [12] Jinke Li, Jiarui Yu, Chenxing Wei, Hande Dong, Qiang Lin, Liangjing Yang, Zhicai Wang, and Yanbin Hao. Unisvg: A unified dataset for vector graphic understanding and generation with multimodal large language models. In *Proceedings of the 33rd ACM International Conference on Multimedia*, pages 13156–13163, 2025. [1](#), [2](#), [4.1](#), [A.2](#)
- [13] Lei Li, Yuancheng Wei, Zhihui Xie, Xuqing Yang, Yifan Song, Peiyi Wang, Chenxin An, Tianyu Liu, Sujian Li, Bill Yuchen Lin, et al. Vl-rewardbench: A challenging benchmark for vision-language generative reward models. In *Proceedings of the Computer Vision and Pattern Recognition Conference*, pages 24657–24668, 2025. [3.3](#)
- [14] Renhao Li, Jianhong Tu, Yang Su, Hamid Alinejad-Rokny, Derek F Wong, Junyang Lin, and Min Yang. One model to critique them all: Rewarding agentic tool-use via efficient reasoning. *arXiv preprint arXiv:2510.26167*, 2025. [2](#)
- [15] Jun Ling, Yao Qi, Tao Huang, Shibo Zhou, Yanqin Huang, Jiang Yang, Ziqi Song, Ying Zhou, Yang Yang, Heng Tao Shen, et al. Table2latex-rl: High-fidelity latex code generation from table images via reinforced multimodal language models. *arXiv preprint arXiv:2509.17589*, 2025. [1](#), [2](#)
- [16] Ziyu Liu, Zeyi Sun, Yuhang Zang, Xiaoyi Dong, Yuhang Cao, Haodong Duan, Dahua Lin, and Jiaqi Wang. Visual-rft: Visual reinforcement fine-tuning. *arXiv preprint arXiv:2503.01785*, 2025. [2](#)
- [17] Ziyu Liu, Yuhang Zang, Shengyuan Ding, Yuhang Cao, Xiaoyi Dong, Haodong Duan, Dahua Lin, and Jiaqi Wang. Spark: Synergistic policy and reward co-evolving framework. *arXiv preprint arXiv:2509.22624*, 2025. [2](#)
- [18] Ahmed Masry, Xuan Long Do, Jia Qing Tan, Shafiq Joty, and Enamul Hoque. Chartqa: A benchmark for question answering about charts with visual and logical reasoning. In *Findings of the association for computational linguistics: ACL 2022*, pages 2263–2279, 2022. [B.1](#)
- [19] Minesh Mathew, Viraj Bagal, Rubèn Tito, Dimosthenis Karatzas, Ernest Valveny, and CV Jawahar. Info-graphicvqa. In *Proceedings of the IEEE/CVF Winter Conference on Applications of Computer Vision*, pages 1697–1706, 2022. [B.1](#)
- [20] Minesh Mathew, Dimosthenis Karatzas, and CV Jawahar. Docvqa: A dataset for vqa on document images. In *Proceedings of the IEEE/CVF winter conference on applications of computer vision*, pages 2200–2209, 2021. [B.1](#)
- [21] Junbo Niu, Zheng Liu, Zhuangcheng Gu, Bin Wang, Linke Ouyang, Zhiyuan Zhao, Tao Chu, Tianyao He, Fan Wu, Qintong Zhang, et al. Mineru2. 5: A decoupled vision-language model for efficient high-resolution document parsing. *arXiv preprint arXiv:2509.22186*, 2025. [1](#), [2](#)
- [22] OpenAI. Openai o3-mini system card, 2025. [1](#)
- [23] Linke Ouyang, Yuan Qu, Hongbin Zhou, Jiawei Zhu, Rui Zhang, Qunshu Lin, Bin Wang, Zhiyuan Zhao, Man Jiang, Xiaomeng Zhao, et al. Omnidocbench: Benchmarking diverse pdf document parsing with comprehensive annotations. In *Proceedings of the Computer Vision and Pattern Recognition Conference*, pages 24838–24848, 2025. [1](#), [4.1](#)
- [24] Hao Peng, Yunjia Qi, Xiaozhi Wang, Zijun Yao, Bin Xu, Lei Hou, and Juanzi Li. Agentic reward modeling: Integrating human preferences with verifiable correctness signals for reliable reward systems. *arXiv preprint arXiv:2502.19328*, 2025. [2](#)

- [25] Jake Poznanski, Aman Rangapur, Jon Borchardt, Jason Dunkelberger, Regan Huff, Daniel Lin, Christopher Wilhelm, Kyle Lo, and Luca Soldaini. olmocr: Unlocking trillions of tokens in pdfs with vision language models. *arXiv preprint arXiv:2502.18443*, 2025. [1](#), [4.1](#)
- [26] Juan A Rodriguez, Shubham Agarwal, Issam H Laradji, Pau Rodriguez, David Vazquez, Christopher Pal, and Marco Pedersoli. Starvector: Generating scalable vector graphics code from images. *arXiv preprint arXiv:2312.11556*, 2023. [A.2](#)
- [27] Zhihong Shao, Peiyi Wang, Qihao Zhu, Runxin Xu, Junxiao Song, Xiao Bi, Haowei Zhang, Mingchuan Zhang, YK Li, Y Wu, et al. Deepseekmath: Pushing the limits of mathematical reasoning in open language models. *arXiv preprint arXiv:2402.03300*, 2024. [2](#), [4.1](#)
- [28] Chenglei Si, Yanzhe Zhang, Ryan Li, Zhengyuan Yang, Ruibo Liu, and Diyi Yang. Design2Code: Benchmarking multimodal code generation for automated front-end engineering. In *ACL*, 2025. [1](#)
- [29] Oriane Siméoni, Huy V Vo, Maximilian Seitzer, Federico Baldassarre, Maxime Oquab, Cijo Jose, Vasil Khali-dov, Marc Szafraniec, Seungeun Yi, Michaël Ramamonjisoa, et al. Dinov3. *arXiv preprint arXiv:2508.10104*, 2025. [2](#)
- [30] Aaditya Singh, Adam Fry, Adam Perelman, Adam Tart, Adi Ganesh, Ahmed El-Kishky, Aidan McLaughlin, Aiden Low, AJ Ostrow, Akhila Ananthram, et al. Openai gpt-5 system card. *arXiv preprint arXiv:2601.03267*, 2025. [3.1](#), [3.3](#)
- [31] Qiushi Sun, Jingyang Gong, Yang Liu, Qiaosheng Chen, Lei Li, Kai Chen, Qipeng Guo, Ben Kao, and Fei Yuan. Januscoder: Towards a foundational visual-programmatic interface for code intelligence. *arXiv preprint arXiv:2510.23538*, 2025. [4.1](#)
- [32] Wentao Tan, Qiong Cao, Chao Xue, Yibing Zhan, Changxing Ding, and Xiaodong He. Chartmaster: Advancing chart-to-code generation with real-world charts and chart similarity reinforcement learning. *arXiv preprint arXiv:2508.17608*, 2025. [1](#), [2](#)
- [33] Yibin Wang, Yuhang Zang, Hao Li, Cheng Jin, and Jiaqi Wang. Unified reward model for multimodal understanding and generation. *arXiv preprint arXiv:2503.05236*, 2025. [2](#)
- [34] Zirui Wang, Mengzhou Xia, Luxi He, Howard Chen, Yitao Liu, Richard Zhu, Kaiqu Liang, Xindi Wu, Haotian Liu, Sadhika Malladi, et al. Charxiv: Charting gaps in realistic chart understanding in multimodal llms. *Advances in Neural Information Processing Systems*, 37:113569–113697, 2024. [B.1](#)
- [35] Cheng Yang, Chufan Shi, Yaxin Liu, Bo Shui, Junjie Wang, Mohan Jing, Linran Xu, Xinyu Zhu, Siheng Li, Yuxiang Zhang, et al. Chartmimic: Evaluating lmm’s cross-modal reasoning capability via chart-to-code generation. *arXiv preprint arXiv:2406.09961*, 2024. [1](#), [4.1](#), [4.2](#)
- [36] Yiying Yang, Wei Cheng, Sijin Chen, Xianfang Zeng, Fukun Yin, Jiayu Zhang, Liao Wang, Gang Yu, Xingjun Ma, and Yu-Gang Jiang. Omnisvg: A unified scalable vector graphics generation model. *arXiv preprint arXiv:2504.06263*, 2025. [2](#)
- [37] Weizhe Yuan, Richard Yuanzhe Pang, Kyunghyun Cho, Sainbayar Sukhbaatar, Jing Xu, and Jason E. Weston. Self-rewarding language models. *ArXiv*, abs/2401.10020, 2024. [2](#)
- [38] Yuhang Zang, Xiaoyi Dong, Pan Zhang, Yuhang Cao, Ziyu Liu, Shengyuan Ding, Shenxi Wu, Yubo Ma, Haodong Duan, Wenwei Zhang, et al. Internlm-xcomposer2. 5-reward: A simple yet effective multi-modal reward model. *arXiv preprint arXiv:2501.12368*, 2025. [2](#)
- [39] Jiarui Zhang, Yuliang Liu, Zijun Wu, Guosheng Pang, Zhili Ye, Yupei Zhong, Junteng Ma, Tao Wei, Haiyang Xu, Weikai Chen, et al. Monkeyocr v1. 5 technical report: Unlocking robust document parsing for complex patterns. *arXiv preprint arXiv:2511.10390*, 2025. [2](#)
- [40] Zhihan Zhang, Yixin Cao, and Lizi Liao. Enhancing chart-to-code generation in multimodal large language models via iterative dual preference learning. *arXiv preprint arXiv:2504.02906*, 2025. [2](#)

- [41] Xuanle Zhao, Deyang Jiang, Zhixiong Zeng, Lei Chen, Haibo Qiu, Jing Huang, Yufeng Zhong, Liming Zheng, Yilin Cao, and Lin Ma. Vincicoder: Unifying multimodal code generation via coarse-to-fine visual reinforcement learning. *arXiv preprint arXiv:2511.00391*, 2025. [1](#), [2](#), [4.1](#), [4.2](#), [A.1](#)
- [42] Xuanle Zhao, Xianzhen Luo, Qi Shi, Chi Chen, Shuo Wang, Zhiyuan Liu, and Maosong Sun. Chartcoder: Advancing multimodal large language model for chart-to-code generation. *arXiv preprint arXiv:2501.06598*, 2025. [1](#), [2](#), [A.2](#)
- [43] Xu Zhong, Elaheh ShafieiBavani, and Antonio Jimeno Yepes. Image-based table recognition: data, model, and evaluation. *arXiv preprint arXiv:1911.10683*, 2019. [2](#)
- [44] Banghua Zhu, Evan Frick, Tianhao Wu, Hanlin Zhu, and Jiantao Jiao. Starling-7b: Improving llm helpfulness & harmlessness with rlaiif, November 2023. [2](#)

## Outline

In the appendix, we provide additional materials to support the main paper and facilitate a deeper understanding of [Visual-ERM](#).

First, in [Sec. A](#), we provide detailed descriptions of the models, datasets, benchmark construction, and experimental setups used throughout the paper, aiming to ensure reproducibility.

Second, [Sec. B](#) presents additional experimental analyses and ablation studies, including evaluations on general VQA benchmarks, investigations of multi-task reward modeling, robustness analyses of different judge models, further studies on reward design, test-time scaling and so on.

Third, in [Sec. C](#), we list the full prompt templates used in our experiments, covering reward model data generation, [Visual-ERM](#) inference across different vision-to-code tasks, and the evaluation protocol of VC-RewardBench.

Finally, [Sec. D](#) provides representative qualitative case studies from chart-to-code, table-to-markdown, and SVG-to-code tasks, illustrating typical visual discrepancies and the fine-grained feedback produced by [Visual-ERM](#).

## A. More Details

### A.1. Models

This work involves multiple models of different roles and scales. For clarity and reproducibility, we summarize the models used throughout the paper and their corresponding usage in each stage of the pipeline.

**Visual-ERM (Reward Model).** We build [Visual-ERM](#) on top of Qwen3-VL-8B-Instruct [2]. While Qwen3-VL-8B-Instruct already exhibits strong multimodal perception and reasoning abilities, we find that it is not a reliable *image-to-image discrepancy* judge out of the box—especially for structured visuals where the key differences are often text- and layout-centric. This limitation is empirically reflected in [Sec. 4.3](#), where the base model shows poor discrimination on fine-grained visual mismatches.

Starting from this 8B backbone, we train [Visual-ERM](#) on a large-scale reward-modeling corpus spanning three vision-to-code domains: Chart-to-Code (104K), Table-to-Markdown (125K), and SVG-to-Code (111K). This training equips [Visual-ERM](#) with task-agnostic yet fine-grained judgment capabilities. Notably, despite its relatively small size, [Visual-ERM](#) substantially outperforms Qwen3-VL-235B-Instruct as a judge and achieves performance competitive with strong proprietary models, demonstrating that targeted reward model training can be more effective than simply scaling up a general-purpose LLM.

**Policy models for RL.** For reinforcement learning, we consider two types of policy backbones. The first is Qwen3-VL-8B-Instruct, which serves as our default policy model across tasks. In this setting, we use [Visual-ERM](#) as the reward model and optimize Qwen3-VL-8B-Instruct with RL to improve its vision-to-code generation quality.

In addition, to test whether [Visual-ERM](#) can also improve stronger specialized parsers, we use VinciCoder-8B-SFT [41] as an alternative policy backbone on Chart-to-Code and SVG-to-Code. VinciCoder-8B-SFT provides a stronger supervised baseline for these tasks, and applying [Visual-ERM](#)-guided RL on top of it allows us to evaluate the reward model’s transferability and its ability to refine already-competitive policies.

For Table-to-Markdown, we do not include VinciCoder-8B-SFT because it does not have a comparable task-specific SFT baseline for tables; therefore, we only use Qwen3-VL-8B-Instruct as the policy model for RL in this setting.

### A.2. Datasets

We use multiple datasets throughout the paper for reward-model training, RL policy optimization, and benchmark construction. For completeness, we summarize them here. The annotations and training data will be released publicly in the future, and qualitative examples are provided in [Sec. D](#).

**Reward-model training data.** We first collect a pool of images and their corresponding ground-truth annotations from public vision-to-code datasets spanning charts, tables, and SVG-style graphics [5, 10, 12, 26, 42]. However, these raw pairs are not directly suitable for training a reward model, because Visual-ERM requires supervision on *image-to-image discrepancies* rather than only paired input-output examples. We therefore construct training instances by synthesizing realistic error patterns and converting them into *rendered* visual differences.

Concretely, we create imperfect predictions via two complementary routes: (i) *error injection* on ground-truth annotations using a strong yet cost-effective model (GPT-5-mini) as well as Qwen3-VL-235B-Instruct, and (ii) *model-generated predictions* by running Qwen3-VL-8B-Instruct on a subset of ground-truth images to obtain naturally occurring parsing errors. We then render each prediction back into an image, forming an (Original Image, Generated Image) pair that reflects the types of distortions encountered in practice. Given each image pair, we use GPT-5-mini to produce structured annotations, including fine-grained error descriptions (category, location, severity), as illustrated in Sec. D. This procedure yields three reward-modeling datasets: 104K instances for Chart-to-Code, 125K for Table-to-Markdown, and 111K for SVG-to-Code.

**RL training data.** The RL data are drawn from the same underlying sources, but require substantially less processing. Unlike reward-model training, RL does not require free-form error annotations: during training, Visual-ERM directly compares the original image with the re-rendered prediction and outputs an image-to-image reward. As a result, we only need the ground-truth images, and in many cases the ground-truth parsing text is not necessary. In our experiments, we use 11K images for Chart-to-Code RL, 40K for Table-to-Markdown RL, and 10K for SVG-to-Code RL.

**VC-RewardBench construction data.** We construct VC-RewardBench using a similar discrepancy-centric philosophy, but with substantially stricter quality control to ensure reliability as an evaluation benchmark. We begin with a candidate pool of 4.5K image pairs and obtain annotations from three state-of-the-art proprietary models: GPT-5-mini, Gemini2.5-Pro, and Gemini3-Pro. We then manually consolidate, filter, and curate the collected annotations to resolve inconsistencies and remove ambiguous or low-quality cases. The final benchmark contains 1,335 carefully vetted examples, which we use to evaluate fine-grained image-to-image judging ability in structured visual domains.

### A.3. VC-RewardBench Statistics

This section reports detailed statistics of VC-RewardBench. The benchmark contains 1,335 curated examples spanning three structured-visual domains: 595 chart instances, 442 SVG instances, and 298 table instances.

Beyond instance counts, VC-RewardBench provides fine-grained error annotations that characterize the discrepancy types between the original image and the re-rendered prediction. For the chart subset, the annotations include 231 `text_error`, 619 `style_error`, 462 `data_error`, and 62 `structure_error`. For the table subset, we annotate 884 `text_error`, 284 `numeric_error`, and 185 `layout_error`. For the SVG subset, the error annotations contain 151 `style_error`, 218 `structure_error`, 360 `shape_error`, and 12 `text_symbol_error`.

Overall, these statistics indicate that VC-RewardBench covers a diverse range of realistic failure modes. In particular, chart examples are dominated by style- and data-related discrepancies, tables primarily exhibit text-centric recognition errors with a non-trivial portion of numeric and layout issues, and SVG examples emphasize geometric `shape_error` and structural composition mismatches. This diversity makes VC-RewardBench a challenging and diagnostic benchmark for evaluating fine-grained image-to-image judging capability.

### A.4. Experimental Setups

We implement supervised training and RL fine-tuning using LLaMA-Factory and the VERL framework. For training Visual-ERM, we use a learning rate of  $1 \times 10^{-5}$  with a batch size of 32. We train for 3 epochs over the reward-modeling dataset. For reinforcement learning, we adopt GRPO with a learning rate of  $1 \times 10^{-6}$  and a batch size of 256. For each prompt, we sample 8 rollouts per GRPO update step to estimate the policy gradients.

**Table 6: Results on general VQA benchmarks.** We evaluate the policy model trained with [Visual-ERM](#)-guided RL on multiple general-purpose benchmarks (with an emphasis on chart- and document-centric VQA) to examine whether its improved vision-to-code performance comes at the cost of general multimodal capability.

Models	ChartQA_TEST	CharXiv_DQ	CharXiv_RQ	DocVQA_VAL	InfoVQA_VAL	AVG
Qwen3-VL-8B-Instruct	82.9	83.8	46.0	95.6	83.1	78.3
+ RL on Chart-to-Code	82.6	83.5	47.2	95.6	83.1	78.4
+ RL on Table-to-Markdown	81.5	83.8	46.7	95.5	83.1	78.1
+ RL on SVG-to-Code	83.2	83.5	46.4	95.8	83.6	78.5

Model	Chart			Table			SVG			AVG		
	$F1_h$	$F1_s$	$S_c$									
<i>Visual-ERM</i>												
+ Chart-Data-Only	40.1	42.6	58.1	17.2	20.4	10.5	11.3	15.3	50.1	26.3	29.3	23.7
+ Table-Data-Only	17.1	20.1	49.3	53.6	54.9	68.8	14.1	19.0	55.2	31.7	34.2	56.6
+ SVG-Data-Only	16.4	21.0	56.0	11.4	17.6	37.0	26.4	31.0	57.3	17.5	22.6	44.2
+ Mix-Data	39.9	42.8	61.2	56.4	57.6	74.8	28.3	32.6	59.6	42.1	44.7	58.4

**Table 7: Effect of Multi-Task Data Mixing.** We compare reward models trained on mixed multi-task data vs. single-task data.

## B. Additional Experimental Analyses

### B.1. Evaluation on General VQA Benchmarks

While [Visual-ERM](#) substantially improves the policy model on a diverse set of vision-to-code tasks, it is important to examine whether these gains come with any trade-offs on broader multimodal capabilities. In particular, reinforcement learning with task-specific rewards may induce distributional shifts or over-specialization, potentially degrading performance on general-purpose visual question answering (VQA) benchmarks.

To assess the generality of the learned policy, we evaluate the RL-trained model on a suite of established VQA benchmarks that are closely related to the structured visual domains considered in this work. Concretely, we select multiple chart- and document-centric benchmarks that require fine-grained visual perception, text recognition, and cross-modal reasoning, thereby serving as a diagnostic for whether [Visual-ERM](#)-guided optimization preserves general visual understanding skills beyond code generation. These benchmarks include ChartQA [18], CharXiv\_DQ [34], CharXiv\_RQ [34], DocVQA [20] and InfoVQA [19].

Tab. 6 summarizes the results. Overall, [Visual-ERM](#)-guided RL does not degrade general VQA performance: the average score remains essentially stable and even shows slight improvements for two of the three RL policies. Concretely, compared to the base Qwen3-VL-8B-Instruct (AVG 78.3), RL on Chart-to-Code reaches 78.4 (+0.1) and RL on SVG-to-Code reaches 78.5 (+0.2), while RL on Table-to-Markdown is comparable at 78.1 (-0.2). At the benchmark level, the most consistent change is on CharXiv-RQ, where all RL variants improve over the base (46.0  $\rightarrow$  47.2 / 46.7 / 46.4), suggesting better fine-grained reasoning over chart-centric queries. Meanwhile, document-centric performance is preserved: DocVQA remains nearly unchanged (95.6  $\rightarrow$  95.6 / 95.5 / 95.8), and InfoVQA is stable with a small gain for the SVG RL policy (83.1  $\rightarrow$  83.6). These results indicate that the gains on vision-to-code do not arise from sacrificing general multimodal competence; instead, [Visual-ERM](#) provides a largely non-destructive learning signal that improves structured visual parsing while maintaining broad chart/document understanding.

### B.2. Evaluation on Effect of Multi-Task Data Mixing

#### B.2.1. Effect of Multi-Task Data Mixing on VC-RewardBench

[Visual-ERM](#) is trained to support multiple tasks that share partial failure modes but also exhibit task-specific characteristics. To examine whether joint training on mixed data is beneficial or induces negative transfer, we ablate the reward model’s training data composition by comparing a unified model trained on all three data sources with task-specific variants trained on a single data type. Results on VC-RewardBench are reported in Tab. 7.

Mixing chart, table, and SVG data yields the best overall performance. We attribute this to cross-task transfer of error patterns (e.g., recognition and layout behaviors learned from tables can generalize to charts due to

**Table 8: Ablation Study of Multi-Task Data Mixing.** We perform RL on the table parsing task using different reward models: one reward model is trained only on table data, while the other reward model is jointly trained on table, chart, and SVG data. TEDS-S denotes TEDS-Structure-Only, and TA represents the table subtask of olmOCRBench. For Edit-Dist, where lower values indicate better performance, we use  $(100 - \text{Edit-Dist})$  when computing the Average.

Model	OmniDocBench			OmniDocBench-v1.5			olmOCRBench	Avg $\uparrow$
	TEDS $\uparrow$	TEDS-S $\uparrow$	Edit-Dist $\downarrow$	TEDS $\uparrow$	TEDS-S $\uparrow$	Edit-Dist $\downarrow$	TA $\uparrow$	
<i>Baseline</i>								
Qwen3-VL-8B-Instruct	78.9	83.9	23.2	72.7	77.2	26.9	75.3	76.8
<i>RL with Different Reward Model</i>								
+ RM (table-data-only)	79.5	84.4	21.6	74.4	79.4	25.0	79.4	78.6
$\Delta$	+0.6	+0.5	+1.6	+1.7	+2.2	+1.9	4.1	+1.8
+ RM (mix-data, Visual-ERM)	81.4	86.3	20.7	75.4	80.4	24.2	78.1	79.5
$\Delta$	+2.5	+2.4	+2.5	+2.7	+3.2	+2.7	+2.8	+2.7

overlapping failure modes) leading to a mutually beneficial effect under joint training. In Sec. B.2.2, we further validate this finding by comparing the downstream RL performance of reward models trained on different data sources.

As shown in Tab. 7, reward models trained on single-task data exhibit a strong task bias. For example, Chart-Data-Only performs well on the Chart subtask ( $F1_h = 40.1$ ,  $F1_s = 42.6$ ), but performs much worse on Table and SVG tasks (e.g., Table  $F1_h = 17.2$ , SVG  $F1_h = 11.3$ ). Similarly, although Table-Data-Only achieves strong results on the Table subtask ( $F1_h = 53.6$ ,  $S_c = 68.8$ ), it generalizes poorly to Chart ( $F1_h = 17.1$ ). In contrast, the mixed-data RM (Mix-Data) achieves more balanced and consistently strong performance across all three task categories. It maintains nearly the same performance on Chart ( $F1_h = 39.9$  vs. 40.1), while significantly improving on Table and SVG (Table:  $F1_h = 56.4$ , SVG:  $F1_h = 28.3$ ). As a result, it attains the best average performance (AVG:  $F1_h = 42.1$ ,  $F1_s = 44.7$ ,  $S_c = 58.4$ ). These results indicate that multi-task training does not introduce obvious negative transfer; instead, it provides positive transfer by sharing structured understanding and code generation abilities, leading to a more generalizable reward model.

### B.2.2. Effect of Multi-Task Data Mixing on RL

To further validate this phenomenon in a practical setting, we apply RMs trained with different datasets to actual RL training and evaluate the effects in real usage. We select the Table-to-Markdown task for this experiment, and the results are shown in Tab. 8. As shown in Tab. 8, both the Table-only RM and the mixed-data RM lead to stable improvements in the Table-to-Markdown RL scenario. Compared with the baseline, RM (table-data-only) improves TEDS and TEDS-S on both benchmarks and reduces Edit-Dist, resulting in an overall average gain of +1.8. More importantly, the mixed-data RM achieves further improvements over the single-task RM on most metrics. On OmniDocBench, it reaches  $TEDS = 81.4$  and  $TEDS-S = 86.3$ , while further reducing Edit-Dist to 20.7. On olmOCRBench-v1.5, it also achieves higher TEDS/TEDS-S and lower Edit-Dist. Overall, it yields an average improvement of +2.7. Although the mixed RM shows a slight drop on the TA metric compared to the Table-only RM (78.1 vs. 79.4), the overall gains are larger, suggesting that a richer multi-task reward signal provides a more robust optimization direction for RL, improving both final performance and generalization on real Table-to-Markdown tasks.

### B.3. Ablation on Different Judge Models

VC-RewardBench evaluates a reward model’s ability to identify fine-grained image-to-image discrepancies and vision-to-code reconstruction errors. In addition to objective metrics (e.g., scalar scores, types and severity), VC-RewardBench also includes *free-form* discrepancy descriptions. Since these descriptions are open-ended and may use different wording to refer to the same underlying issue, an exact string match is insufficient for reliable evaluation.

**LLM-assisted matching protocol.** To evaluate such free-form outputs in a scalable and consistent manner, we employ an LLM-as-Judge to perform *error-level alignment* between the reward model’s predicted error list and the ground-truth error list. Specifically, given the predicted errors and the annotated errors, the judge determines

**Table 9: Ablation on LLM Judges.** VC-RewardBench uses LLM-assisted judging to verify answer correctness. To assess the robustness of this evaluation protocol, we compare multiple LLM-as-Judge models and report the resulting consistency across judges.

Judge	Chart			Table			SVG			AVG		
	$F1_h$	$F1_s$	$S_c$									
GPT-5-mini	39.9	42.8	61.2	56.4	57.6	74.8	28.3	32.6	59.6	42.1	44.7	58.4
GPT-5.2	40.9	45.4	61.2	55.0	57.1	74.8	24.5	31.6	59.6	40.8	45.1	58.4
Gemini2.5-Pro	40.8	42.1	61.2	54.8	55.7	74.8	27.1	28.7	59.6	41.2	42.4	58.4
Gemini3-Flash	41.5	43.7	61.2	56.5	57.8	74.8	28.5	32.1	59.6	43.0	44.9	58.4

**Table 10: Ablation Study of Reward Design.** RSR denotes the Render-Success Reward. TEDS-S denotes TEDS-Structure-Only, and TA represents the table subtask of olmOCRBench. For Edit-Dist, where lower values indicate better performance, we use  $(100 - \text{Edit-Dist})$  when computing the Average.

Model	OmniDocBench			OmniDocBench-v1.5			olmOCRBench	Avg $\uparrow$
	TEDS $\uparrow$	TEDS-S $\uparrow$	Edit-Dist $\downarrow$	TEDS $\uparrow$	TEDS-S $\uparrow$	Edit-Dist $\downarrow$	TA $\uparrow$	
Qwen3-VL-8B-Instruct	78.9	83.9	23.2	72.7	77.2	26.9	75.3	76.8
GRPO (w/o RSR)	80.9	85.6	21.8	75.2	79.9	25.9	79.0	79.0
GRPO (w RSR)	81.4	86.3	20.7	75.4	80.4	24.2	78.1	79.5

for each predicted item whether it (i) correctly matches a ground-truth error, (ii) is a hallucinated/unsupported claim, or (iii) corresponds to an error that exists but is described incorrectly. Symmetrically, the judge also identifies ground-truth errors that are missed by the model. Based on this alignment, we compute two variants of F1: (i) a strict matching criterion ( $F1_h$ , *hard*) that requires close semantic and attribute-level agreement, and (ii) a relaxed criterion ( $F1_s$ , *soft*) that tolerates minor paraphrases or partial matches, reflecting a more lenient notion of equivalence.

**Why judge ablations matter.** Using an LLM introduces a potential dependency on the judge’s calibration and reasoning style. However, in VC-RewardBench the judge is only asked to perform relatively constrained *matching* (rather than open-ended preference ranking), which we hypothesize to be less sensitive to the specific judge model. To validate this, we rerun the same Visual-ERM predictions on VC-RewardBench while varying the judge among several widely-used API models, and report the resulting scores in Tab. 9.

**Results and analysis.** Tab. 9 shows that the evaluation is highly stable across judges. First, the  $S_c$  is identical for all judges (e.g., Chart: 61.2, Table: 74.8, SVG: 59.6, AVG: 58.4), as expected since it is computed deterministically and does not rely on the LLM matcher. Second, the judge-dependent metrics ( $F1_h$  and  $F1_s$ ) vary only modestly: on average,  $F1_h$  ranges from 40.8 to 43.0 (a span of 2.2 points) and  $F1_s$  ranges from 42.4 to 45.1 (a span of 2.7 points) across all judges. At the task level, the variability remains limited—for instance, Table  $F1_s$  ranges from 55.7 to 57.8—indicating that different judges largely agree on which predicted errors are correct versus hallucinated or missing.

Overall, these results suggest that VC-RewardBench is not overly sensitive to the choice of LLM judge. Since the judge is used for structured error-to-error matching under well-specified criteria, replacing the judge model yields consistent conclusions, supporting the robustness of our evaluation protocol.

#### B.4. Ablation Study on Reward Design

We investigate two reward designs. The first directly uses the scalar score produced by the reward model as the reward signal. To improve training stability, the second design augments the reward with an additional render-success reward that indicates whether the generated output can be successfully rendered, which is similar to format reward. To combine the render-success reward with the reward-model score in a principled manner, we further apply score normalization before aggregation.

We conduct an ablation study comparing these two reward formulations, and report the results in Tab. 10. Overall, both designs yield comparable performance gains. Reward design with render-success part achieves a

## Prompt for Distillation Reward Modeling Datasets (Chart) — Part I

You are an **Experienced Specialist for Data Visualization**. You will be provided with **two images**:

- Original Image**: a chart rendered using ground-truth Matplotlib code.
- Generated Image**: a chart rendered using AI-generated Matplotlib code for the **Original Image**.

Your task is to **compare the Generated Image against the Original Image** and identify **all visual discrepancies** that affect:

- correctness of the data,
- layout / structure, or
- aesthetic consistency (when it impacts readability or overall fidelity).

You are evaluating **only what is visible in the two images**, not the underlying code.

---

**Step 1: Compare the two images**  
Carefully compare the Original and Generated images:

- Look at chart types, subplots, axes, data shapes, colors, legends, labels, ticks, and annotations.
- Focus on differences that a developer would need to fix in their Matplotlib code.

If there is **no meaningful difference** between the two images (ignoring tiny pixel-level differences such as anti-aliasing), then you should report **zero errors**.

---

**Step 2: Classify each discrepancy into one category**  
For **every discrepancy you find**, assign it to **exactly one** of the following categories:

**A. `structure\_error` (Layout & Chart Type)**  
**Definition:** Problems with the overall structure or composition of the figure.  
**Typical cases:**

- Wrong chart type (e.g., pie vs. donut, bar vs. line, radar vs. line).
- Wrong number of subplots (e.g., 1 subplot instead of 2).
- Subplots arranged in wrong rows/columns or in the wrong positions.
- Subplots missing or extra.
- Axes that should be shared/aligned in the Original are not shared/aligned in the Generated (or vice versa).

**B. `data\_error` (Content & Geometry)**  
**Definition:** The visualized data itself is incorrect or distorted.  
**Typical cases:**

- Geometry mismatch:** The shape of the curve, polygon, or bar pattern is clearly different (e.g., an increasing line becomes flat or decreasing).
- Value distortion:** Bar heights, pie slice angles, or point positions do not match the original trend or relative ratios.
- Scale / limits mismatch:** Different xlim/ylim or axis scales that significantly change how the data appears.
- Missing / extra data:** Missing series, hallucinated extra lines, wrong number of groups or categories.

**C. `text\_error` (Labels & Annotations)**  
**Definition:** Problems with any visible text in the chart.  
Text includes: titles, subtitles, axis labels, tick labels, legend text, annotations, and text boxes.  
**Typical cases:**

- Missing or incorrect titles, axis labels, tick labels, or legend entries.
- Misplaced labels (e.g., attached to the wrong axis, wrong subplot, or wrong data series).
- Text overlapping with other elements in a way that harms readability.
- Obvious typos or formatting differences that clearly reduce readability (e.g., extremely small font where the original is normal).

**D. `style\_error` (Aesthetics & Appearance)**  
**Definition:** Visual style differences that may not directly change the data values, but affect the overall look and clarity.  
**Typical cases:**

- Color mismatch:** Different color palette or clearly wrong color mapping for data series / categories.
- Markers & lines:** Wrong line style (dashed vs. solid), marker shape, or line width.
- Grid / background:** Missing or extra gridlines, wrong background color, frame visibility changes.
- Other stylistic differences that noticeably change the visual appearance, even if the data is still correct.

---

**Step 3: Assign severity for each error**  
For each error, assign a **severity**:

- 1 (Minor):** Purely aesthetic or very small differences. The chart remains correct and easy to understand (e.g., slightly different shade of color, small font size difference that doesn't hurt readability).
- 2 (Moderate):** Affects readability or requires correction for confident use (e.g., missing axis label, legend partially blocking data, noticeably confusing color choices).
- 3 (Critical):** The chart is **factually wrong or structurally broken**, or seriously misleading (e.g., wrong chart type, missing subplot, reversed trend, wrong scale that changes interpretation, missing key data series).

---

**Figure 6: Prompt for distillation.** The prompt used to distill GPT-5-mini to construct reward-modeling training data for Visual-ERM. We show the Chart-specific prompt here; due to its length, this table includes only the first part.

```

Prompt for Distillation Reward Modeling Datasets (Chart) — Part2

### Step 4: Output format (very important)
You must output ONLY a single valid JSON object, with no additional text, no explanations, and no Markdown code fences.

Use exactly this JSON schema:
{
  "structure_error_count": int,
  "data_error_count": int,
  "text_error_count": int,
  "style_error_count": int,
  "errors": [
    {
      "category": "structure_error | data_error | text_error | style_error",
      "severity": 1 | 2 | 3,
      "location": "Specific location (e.g., 'Left subplot title', 'Red line data', 'Legend')",
      "description": "Concise description of the error."
    }
  ]
}

Additional constraints:
1. If a category has no errors, its _error_count must be 0.
2. The errors list can be empty if the Generated Image is visually consistent with the Original Image (ignoring tiny pixel-level differences).
3. The numeric counts (_error_count) must exactly match the number of errors you report for each corresponding category in the errors list.

```

**Figure 7: Prompt for distillation.** The prompt used to distill GPT-5-mini to construct reward-modeling training data for Visual-ERM. We show the Chart-specific prompt here; due to its length, this table includes only the second part.

Model	UniSVG (ISVGEN)			
	SSIM $\uparrow$	LPIPS $\downarrow$	CLIP $\uparrow$	Score $\uparrow$
Qwen3-VL-8B-Instruct	60.9	60.0	73.3	64.2
+ Reflection (Visual-ERM)	60.4	58.1	74.6	65.2
Qwen3-VL-8B-Instruct (+RL on Visual-ERM)	64.3	49.7	77.5	69.4
+ Reflection (Visual-ERM)	63.9	49.2	78.1	69.8

**Table 11: Test-Time Scaling on SVG-to-Code.** We evaluate TTS on the SVG-to-Code task. Leveraging Visual-ERM as an evaluator, the model performs multiple rounds of self-reflection and revision, leading to improved parsing performance.

slightly larger improvement, which we attribute to its enhanced training stability.

### B.5. More Test-Time Scaling Results

In the main paper, we evaluate reflection-based test-time scaling (TTS) on Chart-to-Code. To further validate the effectiveness and generality of this inference-time refinement strategy, we additionally conduct TTS experiments on SVG-to-Code, with results reported in Tab. 11. We report SSIM and CLIPScore (higher is better) and LPIPS (lower is better).

The table contains two independent comparisons. The first compares Qwen3-VL-8B-Instruct with and without Visual-ERM-guided reflection. Reflection yields consistent improvements across all metrics: CLIPScore increases from 73.3 to 74.6, SSIM remains comparable (60.9 vs. 60.4), and LPIPS decreases from 60.0 to 58.1 (improved). Overall, the aggregated score improves from 64.2 to 65.2 (+1.0), demonstrating that Visual-ERM can provide actionable feedback for inference-time refinement even without RL.

The second comparison evaluates TTS on the Visual-ERM-guided RL policy (Qwen3-VL-8B-Instruct + RL on Visual-ERM). In this setting, applying reflection further boosts performance: LPIPS stays essentially stable (49.7 vs. 49.2, improved), and CLIPScore increases from 77.5 to 78.1. The overall score rises from 69.4 to 69.8 (+0.4). These results indicate that reflection provides additional gains on top of RL, and the RL-trained policy benefits from a stronger starting point, achieving the best absolute performance in both CLIPScore and overall score.

**Table 12: Ablation on the number of reflection rounds in test-time scaling.** We evaluate test-time scaling with different numbers of reflection and revision rounds. The reward model used for providing feedback is [Visual-ERM](#).

Model	ChartMimic v2_direct_600				ChartMimic v2_customized_600				Avg↑
	exec_rate↑	average↑	gpt_score↑	overall↑	exec_rate↑	average↑	gpt_score↑	overall↑	
Qwen3-VL-8B-Instruct (+RL on Visual-ERM)	92.5	74.4	84.6	79.5	91.5	71.8	81.1	76.5	78.0
+ Reflection ( <i>w</i> Visual-ERM) 2 rounds	92.8	75.2	84.5	79.8	92.0	74.4	82.8	78.6	79.2
+ Reflection ( <i>w</i> Visual-ERM) 3 rounds	92.3	74.8	85.8	80.3	94.7	77.1	86.8	82.0	81.1
+ Reflection ( <i>w</i> Visual-ERM) 4 rounds	92.0	74.5	85.4	80.0	94.2	76.9	86.1	81.5	80.7

## B.6. Ablation of the Reflection Rounds in Test-Time Scaling

In our main test-time scaling (TTS) experiments, we use a three-round reflection and revision pipeline by default. To study how the number of reflection rounds affects performance, we conduct an ablation where we vary the number of rounds while keeping the rest of the inference setup identical. Results are summarized in Tab. 12.

Overall, increasing the number of reflection rounds yields consistent improvements, with diminishing returns beyond three rounds. On ChartMimic v2.direct\_600, moving from 2 to 3 rounds improves the overall score from 79.8 to 80.3 (+0.5) and increases the GPT-based metric from 84.5 to 85.8 (+1.3), while keeping `cxcc_rate` and `average` largely stable. On ChartMimic v2.customized\_600, the gains from additional rounds are more pronounced: overall improves from 78.6 (2 rounds) to 82.0 (3 rounds, +3.4) and 81.5 (4 rounds).

Aggregating across both splits, the overall average score increases monotonically from 79.2 (2 rounds) to 81.1 (3 rounds, +1.9) and 80.7 (4 rounds). These results suggest that a moderate number of reflection rounds (3) offers a strong trade-off between performance and inference cost, capturing most of the benefit from iterative refinement while avoiding the diminishing returns observed at 4 rounds.

## C. Prompts

[Visual-ERM](#) relies on several designed prompting templates at multiple stages of the pipeline. Specifically, we use prompts for: (i) distilling GPT-5-mini to construct reward-modeling training data for [Visual-ERM](#), (ii) [Visual-ERM](#) inference across different vision-to-code tasks (Chart-to-Code, Table-to-Markdown, and SVG-to-Code), and (iii) the LLM-assisted judging protocol used in VC-RewardBench for evaluating subjective, free-form error descriptions. We provide the full prompts in this section for reproducibility.

### C.1. Distillation Prompt

To train [Visual-ERM](#), we first build a reward-modeling dataset by distilling GPT-5-mini. Each training instance consists of an *image pair*: an **Original Image** and a **Generated Image** rendered from a candidate output (e.g., model-generated code/markdown). The distillation target is a structured comparison: the model must identify and describe *all visually meaningful discrepancies* between the two images, focusing strictly on what is observable in the rendered results rather than the underlying code.

We construct these image pairs via an automated process that combines (i) *error injection* using a stronger yet cost-effective model (GPT-5-mini) to synthesize diverse, realistic failure patterns, and (ii) *lightweight policy inference* to mimic errors produced by smaller models in practice. The resulting pairs, together with a detailed instruction prompt, are provided to GPT-5-mini to generate high-quality supervision signals for reward modeling. Figures 6 and 7 show the Chart-specific distillation prompt (split into two parts due to length).

**Prompt overview (Chart).** The prompt casts the judge as an “experienced specialist for data visualization” and explicitly defines the evaluation objective: compare the Generated Image against the Original Image and report discrepancies that affect (i) correctness of the data, (ii) layout/structure fidelity, and (iii) visual consistency/readability. Importantly, it instructs the judge to output `zero errors` if no meaningful difference exists.

**Error taxonomy and severity.** To ensure consistent and fine-grained supervision, the prompt requires every discovered discrepancy to be assigned to exactly one of four categories: `structure_error` (layout and chart type),

```

Prompt for Visual-ERM — Chart
PROMPT_CHART2CODE_JUDGEMENT = """"\
You are an Experienced Specialist for Data Visualization. You will be provided with two images:

1. Original Image: a chart rendered using ground-truth Matplotlib code.
2. Generated Image: a chart rendered using AI-generated Matplotlib code for the Original Image.

Your task is to compare the Generated Image against the Original Image and identify all visual discrepancies, then summarize them in a strict JSON format.

Additionally, You should assign a severity score for each error:
- 1 (minor): small errors that barely affect readability or understanding.
- 2 (medium): errors that affect partial understanding and require manual correction for reliable use.
- 3 (severe): structural or key-content errors that break reliable alignment or can significantly mislead.

You MUST output a single JSON object ONLY.
- Do NOT include any extra text.
- The JSON schema MUST match exactly:
{
  "structure_error_count": int,
  "data_error_count": int,
  "text_error_count": int,
  "style_error_count": int,
  "errors": [
    {
      "category": "structure_error | data_error | text_error | style_error",
      "severity": 1 | 2 | 3,
      "location": "Specific location (e.g., 'Left subplot title', 'Red line data', 'Legend')",
      "description": "Concise description of the error."
    }
  ]
}
""""

```

**Figure 8: Visual-ERM inference prompt.** The prompting template used by Visual-ERM at inference time. This prompt is specialized for the Chart-to-Code setting.

*data\_error* (content/geometry and value distortion), *text\_error* (titles, labels, legends, ticks, and annotations), and *style\_error* (aesthetic and appearance). For each error, the judge also assigns a severity level on a three-point scale (minor / moderate / critical), which captures how strongly the discrepancy impacts fidelity or interpretation. This taxonomy is designed to reflect common failure modes in chart rendering and to provide training targets that are both interpretable and actionable.

**Structured JSON output.** Beyond natural-language descriptions, the prompt enforces a strict output format. As shown in Fig. 7, the judge must output **only** a single valid JSON object following a fixed schema, including: (i) per-category error counts, and (ii) an explicit list of error items, each annotated with *category*, *severity*, a localized *location* description (e.g., “legend”, “left subplot title”), and a concise *description*. The prompt additionally specifies consistency constraints (e.g., counts must match the number of listed errors; the error list must be empty when the two images are visually consistent). These constraints substantially reduce annotation ambiguity and make the distilled outputs directly usable for reward-model training and evaluation.

**Why this design.** This prompt design provides two practical benefits. First, it produces *fine-grained* supervision that decomposes visual discrepancies into interpretable components (structure/data/text/style) rather than collapsing them into a single opaque score. Second, the enforced JSON format enables scalable filtering, aggregation, and auditing of the distilled labels, which is critical for building large reward-modeling datasets with reliable quality control.

## C.2. Visual-ERM Inference Prompts

After constructing the distillation dataset, we train our reward model, Visual-ERM, to produce fine-grained, structured feedback for image-to-image visual equivalence. Since this behavior is learned through supervised

```

Prompt for Visual-ERM — Table

PROMPT_TABLE2MARKDOWN_JUDGEMENT = """"\
You are a table parsing quality auditor. You will be given two table images:

- Image 1: the original table screenshot (original)
- Image 2: the parsed / rendered table image (parsed)

Your job is to compare the original vs. parsed images and identify all discrepancies in the parsed table relative to the original,
then summarize them in a strict JSON format.

For every discrepancy, assign exactly ONE of the following categories:
1) layout_error (structure/layout errors)
2) text_error (text recognition errors)
3) numeric_error (numeric/symbol/unit errors)

Assign a severity score for each error:
- 1 (minor): small errors that barely affect readability or understanding
- 2 (medium): errors that affect partial understanding and require manual correction for reliable use
- 3 (severe): structural or key-content errors that break reliable alignment or can significantly mislead

You MUST output a single JSON object ONLY.
- Do NOT include any extra text.
- Do NOT wrap the JSON in markdown code fences like ``` json.
- The JSON schema MUST match exactly:

{
  "layout_error_count": int,
  "text_error_count": int,
  "numeric_error_count": int,
  "errors": [
    {
      "type": "layout_error | text_error | numeric_error",
      "description": "A short description of what is wrong and where it is wrong",
      "severity": 1|2|3
    }
  ]
}
""""

```

**Figure 9: Visual-ERM inference prompt.** The prompting template used by Visual-ERM at inference time. This prompt is specialized for the Table-to-Markdown setting.

fine-tuning, Visual-ERM does not require an overly restrictive prompt at inference time. Instead, we adopt lightweight and efficient prompting templates that primarily (i) specify the comparison setup (Original vs. Generated), (ii) request exhaustive discrepancy discovery conditioned on the task, and (iii) enforce a strict JSON output schema.

We design a task-specific prompt for each vision-to-code setting—Chart-to-Code, Table-to-Markdown, and SVG-to-Code. These prompts share the same overall structure and interface, but differ in the error taxonomy and schema fields to reflect domain-specific failure modes (e.g., chart type/axes/legend for charts, layout and numeric/text errors for tables, and shape/style/text-symbol discrepancies for SVGs). The complete prompts are provided in Fig. 8, Fig. 9, and Fig. 10.

**Chart-to-Code prompt (Fig. 8).** The chart prompt frames Visual-ERM as a data visualization specialist and focuses the comparison on discrepancies that matter for faithful chart reproduction. It explicitly decomposes errors into `structure_error`, `data_error`, `text_error`, and `style_error`, covering (i) global composition (chart type, subplot arrangement, axes sharing), (ii) geometric/value fidelity (bar heights, line trends, point positions, scale mismatches), (iii) textual correctness (titles, tick labels, legends, annotations), and (iv) appearance-level mismatches that may affect readability. This taxonomy is particularly suitable for charts because visually minor differences (e.g., small font changes) can be less important than semantic distortions (e.g., wrong scale or swapped series), and the explicit severity field further encourages Visual-ERM to surface high-impact errors prominently. In practice, the chart prompt also encourages localized descriptions (e.g.,

```

Prompt for Visual-ERM — SVG

PROMPT_IMG2SVG_JUDGEMENT = """"\
You are an expert QA Specialist for Vector Graphics & Icon Generation. You will be provided with two images to compare
visually:

- Image 1 (Ground Truth): The original icon/graphic rendered from correct SVG code.
- Image 2 (Prediction): An icon/graphic rendered from AI-generated SVG code attempting to reproduce Image 1.

Your job is to compare the original vs. parsed images and identify all discrepancies in the parsed image relative to the original,
then summarize them in a strict JSON format.

Assign a severity score for each error:
- 1 (minor): small errors that barely affect readability or understanding
- 2 (medium): errors that affect partial understanding and require manual correction for reliable use
- 3 (severe): structural or key-content errors that break reliable alignment or can significantly mislead

You MUST output a single JSON object ONLY.
- Do NOT include any extra text.
- Do NOT wrap the JSON in markdown code fences like ```json.
- The JSON schema MUST match exactly:

{
  "structure_error_count": int,
  "shape_error_count": int,
  "style_error_count": int,
  "text_symbol_error_count": int,
  "other_error_count": int,
  "errors": [
    {
      "category": "structure_error | shape_error | style_error | text_symbol_error | other_error",
      "severity": 1 | 2 | 3,
      "location": "Visual location (e.g., 'Train Wheel', 'Eye Contour', 'Canvas Background')",
      "description": "Concise description of the visual mismatch."
    }
  ]
}
""""

```

**Figure 10: Visual-ERM inference prompt.** The prompting template used by Visual-ERM at inference time. This prompt is specialized for the SVG-to-Code setting.

“legend”, “x-axis ticks”, “left subplot line”) which makes the feedback more actionable for downstream debugging and revision (such as test-time scaling).

**Table-to-Markdown prompt (Fig. 9).** The table prompt casts Visual-ERM as a table parsing quality auditor and emphasizes structural alignment and textual/numeric accuracy. Compared to charts, tables have less ambiguity in global structure but are highly sensitive to *layout* (row/column spans, merged cells, alignment) and *cell-level content*. Accordingly, the prompt uses a concise three-way categorization: `layout_error`, `text_error`, and `numeric_error`. This design reflects typical failure patterns in table parsing: slight layout shifts can cascade into many downstream cell mismatches, while OCR-style errors often manifest as character substitutions or missing tokens. Separating `numeric_error` from `text_error` is also important in practice, since numerical discrepancies (units, decimal points, sign errors) are often more harmful even when visually subtle. The enforced JSON schema provides a predictable interface for aggregating errors and computing metrics, while keeping the prompt lightweight enough for efficient inference.

**SVG-to-Code prompt (Fig. 10).** The SVG prompt targets vector-graphic reconstruction, where fidelity hinges on geometric primitives and styling attributes. To capture these characteristics, the prompt introduces categories beyond those used for raster-like structured visuals: `shape_error` (incorrect geometry or missing/extraneous components), `style_error` (stroke width, fill, color, opacity), `text_symbol_error` (glyphs, labels, icons) and `structure_error` (global composition and grouping). This taxonomy reflects the fact that SVG failures often involve precise contours and layering, which may not be well described by “data/text/style” alone.

Requiring a location field further encourages spatial grounding, making the output interpretable and enabling targeted correction during RL or test-time scaling.

```

VC-RewardBench Evaluation Prompt

prompt = f"""
You are a strict "error alignment evaluator." Your task is: compare the error list from PRED with the error list from GT,
determine which ones refer to the same specific error point, and output structured JSON.

[Data Category]
{category}

[Allowed Error Types (you may only match within these types)]
{allowed_types}

[Matching Rules (VERY IMPORTANT)]
1) A match is only allowed when pred.type == gt.type OR pred.category == gt.category. Otherwise, it must be judged as not
matching.
2) A "match" requires that the descriptions point to the same specific error point (same location/object/cell/chart element),
and that the error phenomenon is the same or highly consistent.
3) If the pred description is more generalized than gt but clearly refers to the same error point, it can be considered
match_level="partial"; otherwise it is "no".
4) Each pred can match at most one gt, and each gt can match at most one pred (1-to-1 matching).
5) Do not match randomly: it is better to leave unmatched than to make an incorrect match.

[Your output MUST be strictly valid JSON, with no extra text]
The JSON output format is:
{
  "matches": [
    {
      "pred_id": 0,
      "gt_id": 3,
      "match_level": "yes" | "partial"
    }
  ],
  "unmatched_pred": [1, 2],
  "unmatched_gt": [0, 4],
  "notes": "Optional, at most one sentence"
}

[PRED Error List]
{json.dumps(pred_list, ensure_ascii=False, indent=2)}

[GT Error List]
{json.dumps(gt_list, ensure_ascii=False, indent=2)}
"""
.strip()

```

**Figure 11: VC-RewardBench evaluation prompt.** For the subjective, free-form error descriptions in VC-RewardBench, we use an LLM-assisted judge to perform error matching and verification; the prompt used in this evaluation protocol is shown here.

**Common design choices across tasks.** Across all three prompts, we adopt several shared choices that improve usability and robustness: (i) the judge is instructed to compare *only what is visible* in the rendered images, preventing reliance on spurious code cues; (ii) the output must be a *single valid JSON* object with a fixed schema, which reduces post-processing ambiguity and supports scalable training/evaluation; and (iii) the severity score provides a unified notion of error impact, enabling downstream pipelines (e.g., reflection-and-revision) to prioritize the most critical issues first. Together, these prompts serve as a lightweight interface that activates Visual-ERM’s learned capabilities while remaining consistent across heterogeneous vision-to-code domains.

### C.3. VC-RewardBench Evaluation Prompt

A key component of VC-RewardBench is the evaluation of *free-form error descriptions*, which summarize the visual mismatches between the original image and the image re-rendered from the parsed output. Since these

descriptions are subjective and highly open-ended, rule-based string matching is brittle and fails to account for paraphrases, partial matches, or differences in granularity. We therefore use an LLM-as-Judge to perform verification: it determines which predicted errors are correctly matched to ground-truth errors, which are hallucinated, and which are only partially aligned.

Figure 11 shows the prompt used for this evaluation. The prompt is intentionally designed to be *constrained* and *deterministic*: it restricts matching to a predefined set of error types, enforces strict type/category consistency, and requires 1-to-1 alignment between predicted and ground-truth error items. It also explicitly encourages conservative decisions (preferring “unmatched” over uncertain matches) and outputs a single JSON object with match indices and match levels (yes vs. *partial*). These constraints reduce judge arbitrariness and make the resulting metrics more robust across different judge models (as further validated in Tab. 9).

## D. Case Study

### D.1. Data Cases

In this section, we provide representative qualitative examples to illustrate the data format and error annotations used in our pipeline. The reward-model training data and VC-RewardBench examples follow a similar structure—both are built from (Original Image, Re-rendered Image) pairs and accompanied by fine-grained error descriptions. Compared to the training data, VC-RewardBench is labeled by stronger proprietary models and further curated through human filtering, making it more reliable for evaluation. We showcase examples from VC-RewardBench across three domains (Chart, Table, and SVG), as shown in Fig. 12, Fig. 13, and Fig. 14.

**Chart cases (Fig. 12).** The chart examples highlight typical failure modes where textual and structural text are insufficient, and the discrepancies must be judged directly in the rendered space. In the first example, the annotations capture multiple error types: a high-severity `data_error` indicating mismatched bar magnitudes and/or incorrect  $z$ -axis scaling, a `style_error` where the color mapping collapses into a single palette (losing per-category distinction), and a `text_error` that flags unexpected or misplaced labels (e.g., additional axis/title tokens that alter readability). This case demonstrates that visually faithful reconstruction requires jointly preserving data geometry, semantic encodings (color-to-category), and text placement. In the second example, the dominant issues are again `data_error`: the predicted histogram overlays bars incorrectly and uses an inconsistent axis range, which changes the implied distribution. The annotations emphasize that even when the global chart type appears correct, local numeric scaling and bin/value placement errors can lead to critical semantic distortion.

**Table cases (Fig. 13).** The table examples illustrate that errors often concentrate on OCR- and layout-related details, where small differences translate into large structural mistakes in the parsed table. In the first example, the annotations include multiple `text_error` instances on header strings (missing characters, missing units) as well as `numeric_error` cases where punctuation or symbols change the value semantics (e.g., comma vs. dot in decimals, letter O vs. digit 0). Additionally, a high-severity `layout_error` captures column swapping, which is particularly harmful because it can propagate to many cell assignments and invalidate the table schema. In the second example, the errors focus on fine-grained text rendering and alignment: header tokens are misspelled, spacing/formatting changes introduce mismatched column names, and significance markers are rendered inconsistently. The `layout_error` further reflects misalignment of numeric entries across columns, a common structured-visual failure that is hard to detect in the text space but clearly visible after rendering.

**SVG cases (Fig. 14).** The SVG examples emphasize geometry- and structure-centric discrepancies that arise in vector-graphic reconstruction. In the first case, the annotations include `structure_error` due to an extra inner border and an altered frame composition, along with `shape_error` describing changed glyph geometry (stroke thickness and curve profiles) and subtle symbol differences (e.g., rounded vs. rectangular caps). In the second case, the prediction introduces hallucinated protrusions and fails to reproduce continuous elements (e.g., a missing uninterrupted horizontal band), while also exhibiting inconsistent spacing of repeated bars—a combination of `structure_error` and `shape_error`. In the third case, the mismatches include incorrect global composition (outer ring size/placement), an incorrect top-right termination detail, and a mis-centered inner circle, reflecting intertwined `structure_error` and `style_error`. These cases show that SVG fidelity depends critically on precise spatial relationships, path geometry, and layering, which motivates an image-to-image judge that can reason over fine-grained rendered differences.

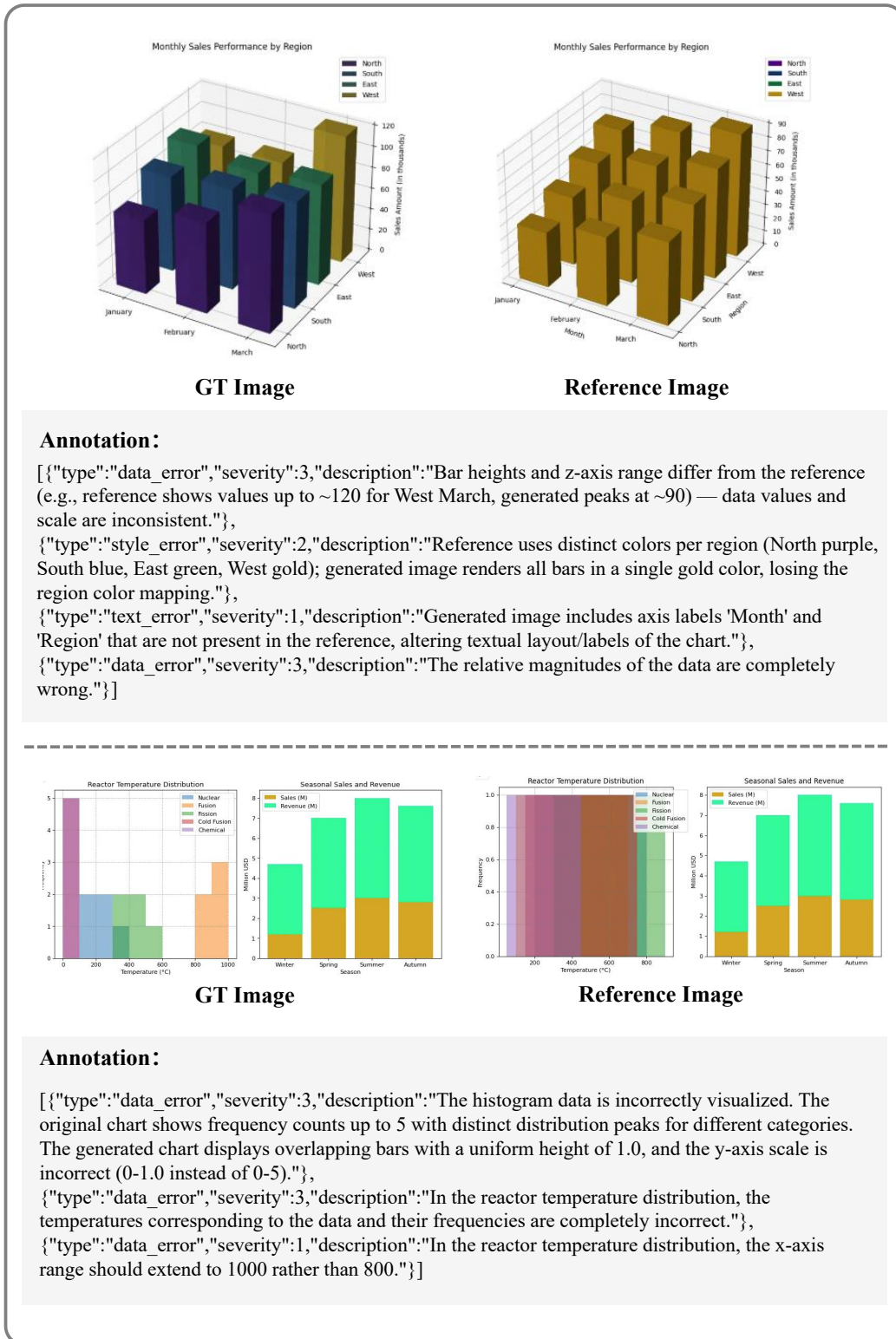


**Figure 12: Case study.** We show representative examples from the Chart-to-Code reward-model training data and the benchmark.

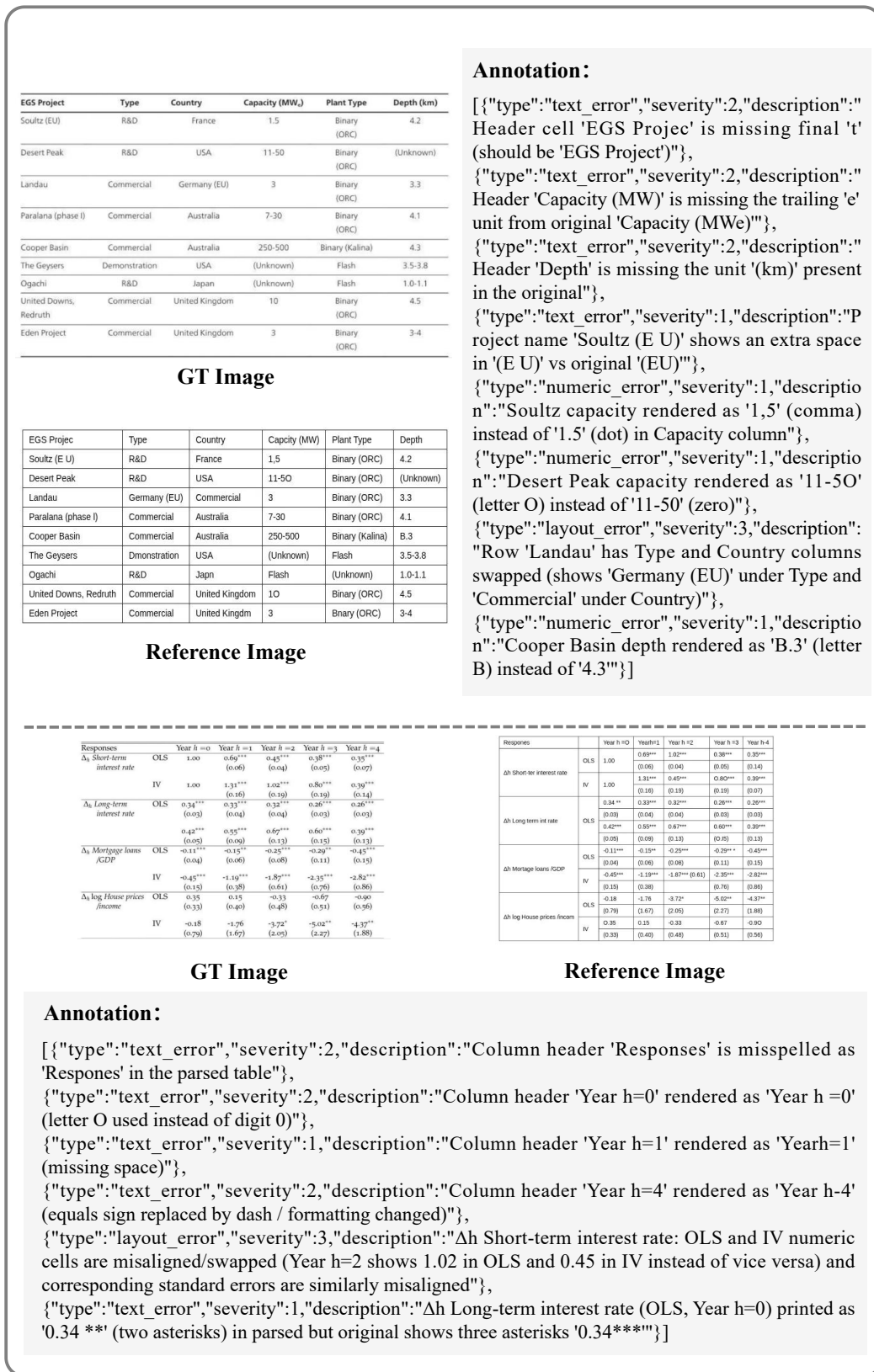
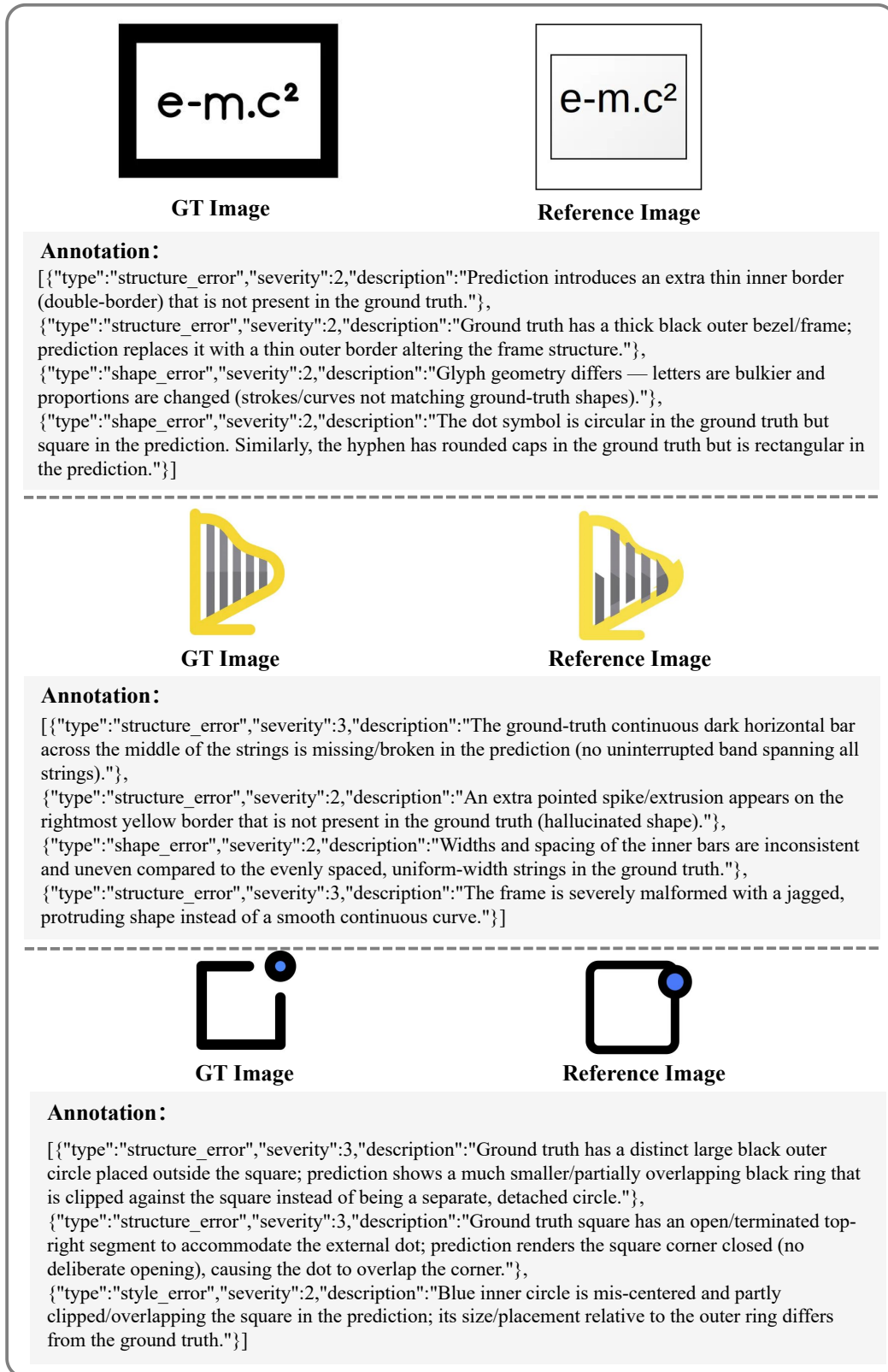


Figure 13: Case study. We show representative examples from the Table-to-Markdown reward-model training data and the benchmark.



**Figure 14: Case study.** We show representative examples from the SVG-to-Code reward-model training data and the benchmark.

Overall, these examples demonstrate that [Visual-ERM](#) and VC-RewardBench captures diverse, realistic discrepancy patterns across domains, and that the error annotations provide interpretable and actionable supervision signals for both training and evaluation.